Sources of salinity and boron in the Gaza strip: Natural contaminant flow in the southern Mediterranean coastal aquifer

Avner Vengosh,[1] Wolfram Kloppmann,[2] Amer Marei,[3] Yakov Livshitz,[4] Alexis Gutierrez,[2] Mazen Banna,[5] Catherine Guerrot,[6] Irena Pankratov,[1] and Hadas Raanan[1]

Received 17 May 2004; revised 26 September 2004; accepted 11 October 2004; published 22 January 2005.

[1] Salinization in coastal aquifers is a global phenomenon resulting from the overexploitation of scarce water resources. The Gaza Strip is one of the most severe cases of salinization, as accelerated degradation of the water quality endangers the present and future water supply for over 1 million people. We investigate the chemical and isotopic ($^{87}Sr/^{86}Sr$, $\delta^{11}B$, $\delta^{18}O$, $\delta^{2}H$, and $\delta^{34}S_{SO4}$) compositions of groundwater from the southern Mediterranean coastal aquifer (Israel) and the Gaza Strip in order to elucidate the origin of salinity and boron contamination. The original salinity in the eastern part of the aquifer is derived from discharge of saline groundwater from the adjacent Avedat aquitard (Na/Cl < 1, $^{87}Sr/^{86}Sr \sim 0.7079$, and $\delta^{11}B \sim 40‰$). As the groundwater flows to the central part of the aquifer, a dramatic change in its composition occurs (Na/Cl > 1, high B/Cl, SO_4/Cl, and HCO_3, $^{87}Sr/^{86}Sr \sim 0.7083$; $\delta^{11}B \sim 48‰$), although the $\delta^{18}O$-$\delta^{2}H$ slope is identical to that of the Avedat aquitard. The geochemical data suggest that dissolution of pedogenic carbonate and gypsum minerals in the overlying loessial sequence generated the Ca-rich solution that triggered base exchange reactions and produced Na- and B-rich groundwater. The geochemical data show that most of the salinization process in the Gaza Strip is derived from the lateral flow of the Na-rich saline groundwater, superimposed with seawater intrusion and anthropogenic nitrate pollution. The methodology of identification of multiple salinity sources can be used to establish a long-term management plan for the Gaza Strip and can also be implemented to understand complex salinization processes in other similarly stressed coastal aquifers.

Citation: Vengosh, A., W. Kloppmann, A. Marei, Y. Livshitz, A. Gutierrez, M. Banna, C. Guerrot, I. Pankratov, and H. Raanan (2005), Sources of salinity and boron in the Gaza strip: Natural contaminant flow in the southern Mediterranean coastal aquifer, *Water Resour. Res.*, *41*, W01013, doi:10.1029/2004WR003344.

1. Introduction

[2] Salinization of coastal aquifers is a global phenomenon that endangers present and future utilization of groundwater resources, particularly in arid and semiarid zones. Understanding the effects of salinization is crucial for water management in regions where groundwater is a diminishing resource and where future urban, agricultural and, consequently, economic development depends exclusively on its availability and quality. In many basins of the Middle East, groundwater resources are shared by more than one state. Water quality degradation in the upstream part of these basins often leads to water stress downstream and thus may lead to regional conflicts. Numerous articles have discussed the political effects of the water shortage in the Middle East, especially in the Gaza Strip [e.g., *Kelly and Homer-Dixon*, 1998; *Ohlsson*, 1995], which is situated on the southern coastal Mediterranean aquifer (Figure 1), because it is perhaps the most extreme example where a population of over one million is totally dependent on groundwater resources [*Moe et al.*, 2001; *Assaf*, 2001]. Human pressure on the coastal aquifer in the Gaza Strip has resulted in the overexploitation beyond natural replenishment and in the significant drawdown of the water levels and continuous degradation of the water quality. For example, the chloride and boron contents in the groundwater exceed in most areas the drinking water limits of 250 mg/L and 1 mg/L, respectively (i.e., the European Union regulations; Figure 2).

[3] In order to be able to break the vicious cycle of extensive exploitation, hydrological deficit, and contamination, the sources and flow paths of contaminates in the aquifer must be elucidated. It is essential to identify the different salinity sources in order to establish in the future a reliable water management plan. The most flagrant example

[1]Department of Geological and Environmental Sciences, Ben-Gurion University of the Negev, Be'er Sheva, Israel.
[2]Service EAU, Bureau de Recherches Géologiques et Minières (BRGM), Orléans, France.
[3]Faculty of Science and Technology, Al Quds University, Jerusalem, West Bank.
[4]Hydrological Service, Jerusalem, Israel.
[5]Palestinian Water Authority, Gaza, Gaza Strip.
[6]Service ANA, Bureau de Recherches Géologiques et Minières (BRGM), Orléans, France.

Copyright 2005 by the American Geophysical Union.
0043-1397/05/2004WR003344$09.00

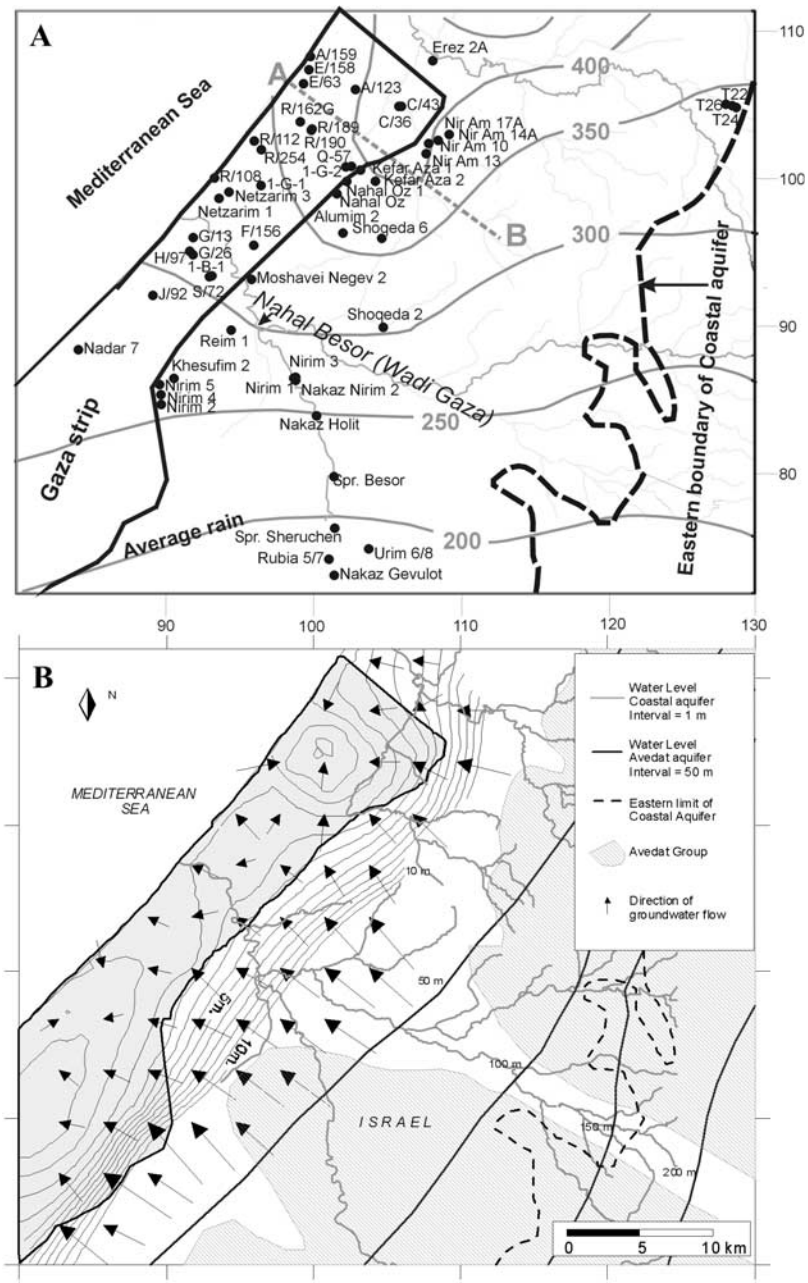

Figure 1. (a) Location map of research wells analyzed in this study on the background of the long-term average values of precipitation isohyet in the region. Dashed line A-B refers to the hydrogeological section (Figure 3). (b) Water level map and groundwater flow directions in the Mediterranean coastal aquifer (fall 1998) and the Avedat aquitard (marked in solid lines). Note the deep hydrological depressions in the northern and southern parts of the Gaza Strip and the general southeast to northwest flow direction. Also note that the eastern margin of the coastal aquifer is located east of the western boundary of the underlying Avedat aquitard, reflecting a direct hydrogeological connection (modified after *Livshitz* [1999]).

of a priori assertions concerning coastal aquifers is to consider seawater intrusion to be the primary salinity source. Moreover, it is commonly believed that merely halting seawater intrusion will solve the aquifer salinity problem [e.g., *Jones et al.*, 1999]. However, many studies have shown that other sources of salinity also affect the water quality of groundwater resources in coastal aquifers [*Maslia and Prowell*, 1990; *Izbicki*, 1991; *Vengosh et al.*, 1999, 2002; *Penny et al.*, 2003]. In the fragile hydropolitical framework within the Gaza Strip, understanding the origin of the salinity has many political and economic implications (e.g., water sharing with Israel, political stability, and economic growth) in addition to direct operational water management.

[4] Tracing the origin of the salinity is not an easy task, particularly in aquifers that may be contaminated from

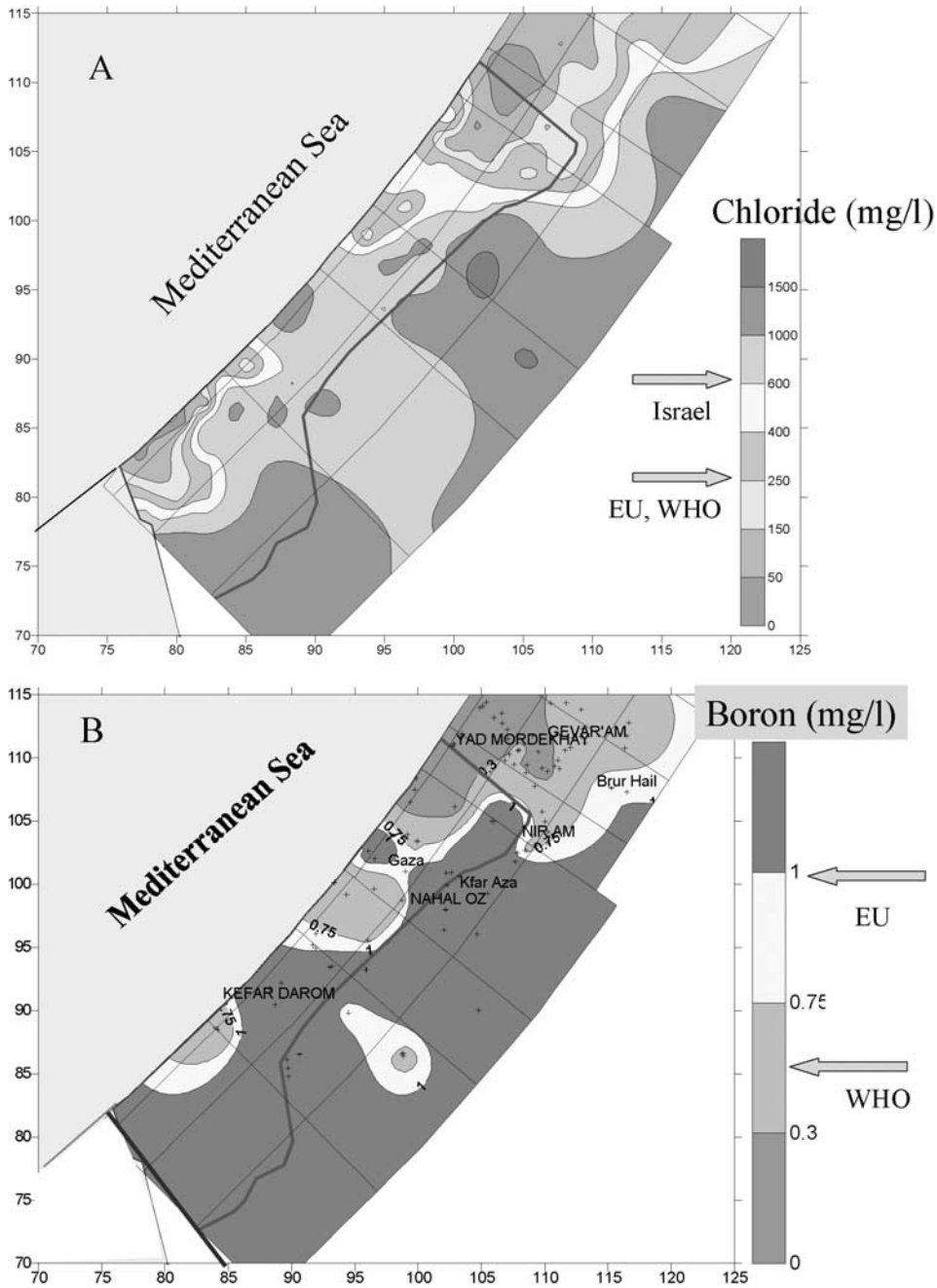

Figure 2. (a) Distribution of chloride concentrations (mg/L) in the southern Mediterranean coastal aquifer and the Gaza Strip as measured in 2000. Arrows indicate upper limits of drinking-water regulations in Israel and the European Union (EU) and recommended by the World Health Organization (WHO). (b) Distribution boron concentrations (mg/L) in the southern Mediterranean coastal aquifer and the Gaza Strip as measured in 2000. Arrows indicate upper limits of drinking water regulations in Israel and the European Union (EU) and recommended by the World Health Organization (WHO). See color version of this figure at back of this issue.

multiple nonpoint saline sources. One of the important elements for tracing salinity sources is the assumption that the chemical compositions of the original saline sources, particularly conservative constituents such as Br/Cl are preserved during the salinization process [*Vengosh*, 2003]. However, additional processes (e.g., water-rock interactions) may hamper the ability to elucidate the original saline sources. Here, we investigated the chemical and isotopic compositions of strontium, boron, oxygen, hydrogen, and sulfur in groundwater from the southern Mediterranean coastal aquifer that is shared between Israel and the Gaza Strip. Using different geochemical and isotopic tracers provides an efficient diagnostic tool for elucidating the origin of the salinity and boron contamination. We show that the predominant salinity source in the southern Mediterranean coastal aquifer is natural inland saline groundwa-

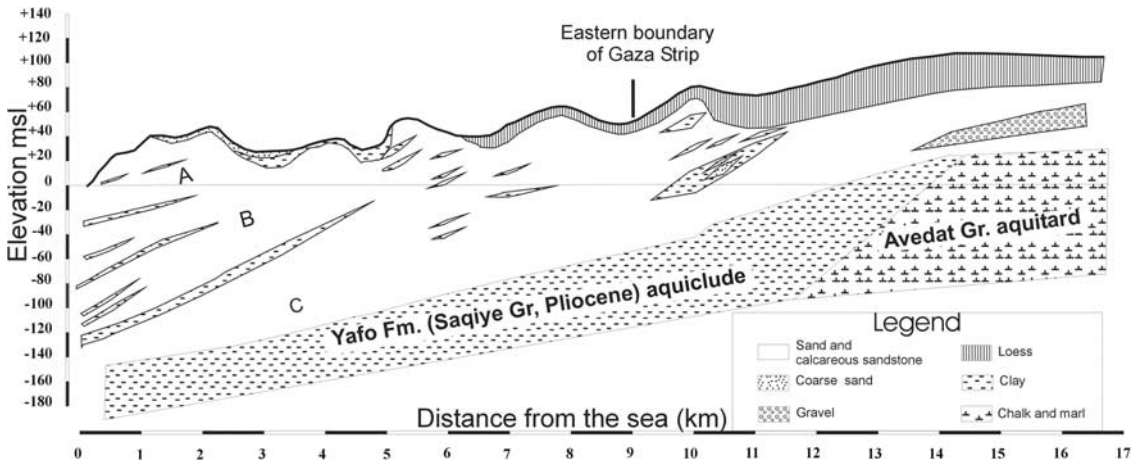

Figure 3. Schematic general hydrogeological SE-NW cross section of the coastal aquifer along line AB in Figure 1a. The cross section was modified after *Tolmach* [1991].

ter that flows from the central aquifer in Israel into the Gaza Strip.

2. Hydrogeology

[5] The Coastal Plain aquifer is located along the Mediterranean coast of Israel and Gaza Strip. It is composed of Pliocene-Pleistocene calcareous sandstone, sands, sandy loam, and clays (Figure 3). The aquifer thickness varies from 200 m in the west near the coast to a few meters at the eastern margins. Up to a distance of 4 to 6 km from the coastline, impermeable layers of clays divide the aquifer into several confined subaquifers (marked as "A" to "C" in Figure 3), whereas in its central and eastern sections the aquifer is undivided and phreatic. The unsaturated zone in the western part of the aquifer is composed of relatively highly permeable sand, calcareous sandstone, and sandy loam. In the eastern part, the aquifer is covered by thick loess soils (up to 20 m depth) of low conductivity. Recharge occurs through the unsaturated zone in areas of sand dunes (central and western aquifer) but is limited in areas of thick layers of loess soils (eastern areas of the aquifer) due to their lower permeability. The amount of precipitation decreases by 50% from the North (about 400 mm) to the South (200 mm) (Figure 1a).

[6] In the western and central areas, the aquifer overlies an aquiclude unit with a thickness of several hundreds of meters, composed of marine shale and marl (the Yafo Formation of the Saqiye Group). Along the eastern margin, the aquifer overlies directly on the Avedat Group (Eocene) aquitard since the Yafo Formation occurs only in the central section of the coastal plain [*Gvirtzman*, 1969; *Livshitz*, 1999] (Figures 1b and 3). The structure and the thickness of the aquifer vary significantly from north to south in the Gaza Strip. In the northern section, the thickness of the aquifer in its western and central area is 180 to 200 m. In the central Gaza Strip the thickness decreases to 140 to 160 m. In the southern part, the thickness of the aquifer is only 100 to 120 m. Along the north-south transition, the basic structure of subaquifer division along the coast is unchanged, but the thickness of the lower subaquifer unit "C" decreases significantly [*Mercado*, 1968; *Fink*, 1992; *Guttman*, 2002].

[7] Historic hydrological data [*Mercado*, 1968; *Fink*, 1992; *Livshitz*, 1999; *Guttman*, 2002] indicate that the natural flow regime was from SE to NW toward the Mediterranean Sea (Figure 1b). This means that part of the recharge of the Gaza groundwater occurs in the East, on the territory of Israel. Over the years the amount of pumping in the Gaza Strip has steeply increased (currently 155 $\times$ 10^6 m^3/y) and is not balanced by natural or anthropogenic replenishments. The natural recharge of the aquifer is estimated to be 35 $\times$ 10^6 m^3/y while the human induced (agricultural return flow and wastewater) is estimated at 52 $\times$ 10^6 m^3/y and lateral inflow from the eastern part of the aquifer is 37 $\times$ 10^6 m^3/y [*Moe et al.*, 2001; *Fink*, 1992]. The Gaza Strip is thus facing an overall annual deficit of about 30 $\times$ 10^6 m^3/y [*Moe et al.*, 2001]. As a result of overpumping, regional water levels were lowered, and two deep hydrological depressions have formed in the urban areas of the Gaza Strip including Gaza City in the North and Rafah in the South (Figure 1b) [*Moe et al.*, 2001; *Mercado*, 1968; *Fink*, 1992; *Melloul and Bibas*, 1992].

[8] The Avedat Group (Eocene) aquitard is composed of low-permeability chalk that has been intensively fractured and jointed. Consequently, the fractured flow controls water recharge and groundwater flow [*Nativ et al.*, 1995; *Nativ and Nissim*, 1992; *Livshitz*, 1999]. Evidence for rapid recharge and transport along fractures is seasonal fluctuations of water levels, high tritium concentration, high rates of contaminants flow, and $\delta^{18}O$ -$\delta^{2}H$ composition that is identical to modern precipitation in the northern Negev [*Nativ et al.*, 1995; *Nativ and Nissim*, 1992]. Hence, although the Eocene chalks are referred to as "aquitard," numerous studies have shown that groundwater flow within the formation is rapid. Although constituted of heterogeneous permeabilities, the Avedat Group is a unit of a continuous water table whose potentiometric surface is about 200 m to 50 m, relative to 10 to 20 m in the eastern part of the coastal aquifer (Figure 1b). Given the potentiometric head difference between the aquitard and the adjacent coastal aquifer (Figure 1b), groundwater flows along this contact [*Nativ and Nissim*, 1992; *Livshitz*, 1999]. *Livshitz* [1999] demonstrated that the chemical composition of groundwater within the Kurkar Group (constituting the coastal aquifer) along the contact zone (Figure 3) mimics

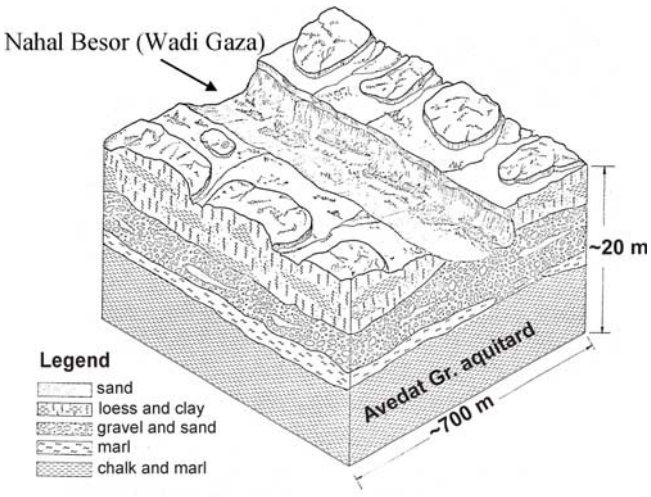

Figure 4. A schematic block-diagram of Nahal Besor (Wadi Gaza) and local hydrogeology. Modified after *Movshoviz* [1979] and *Michaeli and Movshoviz* [1981].

the composition of the Avedat aquitard, indicating a direct flow of groundwater from the fracture chalks into the sandstone of the coastal aquifer.

[9] In the central part of the Gaza Strip (Figure 1) a dried-up river (Nahal Besor in Hebrew or Wadi Gaza in Arabic), which is perennially flooded, cuts into the coastal aquifer. The highly permeable sediments that are associated with the river form an alluvial and shallow aquifer that directly overlies the chalk of Avedat Group aquitard (Figure 4). Elevation of the base of Nahal Besor in the southern part of the research area (Spring Sharuchan, Figure 1a) is about 90 to 100 means sea level below the potentiometric surface of the Avedat Group (Figure 1b), enabling drainage of groundwater from the Avedat Group to the river floor and the shallow alluvial aquifer.

3. Analytical Techniques

[10] Groundwater samples were collected from both Israeli and Palestinian pumping wells (Figure 1a). Water samples were filtered immediately after reaching the laboratory. Loess leaching experiments were performed by batch reaction of double-distilled water with loess soil in 1:1 ratio, centrifuge and filtration of the slurry. The chemical composition of the water was analyzed at the Water Laboratory of Ben-Gurion University; cations and boron were measured by inductively coupled plasma–optical emission spectrometry (ICP-OES), anions were measured by ion chromatography. Analytical errors in all dissolved constituents did not exceed 5%. Boron, strontium, sulfur, oxygen and hydrogen isotopes were measured at BRGM isotope laboratories.

[11] Boron isotopes were determined by positive thermal ionization mass spectrometry [*Spivack and Edmond*, 1986] on a Finnigan MAT 261 solid source mass spectrometer. Waters and dissolved solid salts were run through cationic resin (IR120) in order to remove major ions. Boron isolation was obtained by using the Amberlite IRA-743 boron selective resin according to a method adapted from *Gaillardet and Allègre* [1995]. The sample was then loaded on Ta single filament with Cs and mannitol, and run as $Cs_2BO_2^+$ ion. Values are reported on the δ scale relative to NBS951 boric acid standard where $\delta^{11}B$ (in ‰) is defined as $[\{(^{11}B/^{10}B)_{sample}/(^{11}B/^{10}B)_{standard}\} - 1] \times 10^3$. The $^{11}B/^{10}B$ value obtained for the NBS951 boric acid standard after oxygen correction was 4.05018 ± 0.00125 (2σ, number of determinations = 27). The long-term external reproducibility based on replicate analysis is then ±0.5‰. The internal error is often better than 0.3‰.

[12] Strontium isotope analyses [*Négrel and Deschamps*, 1996] were performed after chemical separation by standard cation exchange chemistry, using a Finnigan MAT 262 multiple collector mass spectrometer and a single W filament with a tantalum activator. The $^{87}Sr/^{86}Sr$ ratios were determined for all the water samples with the total blank for Sr being less than 0.5 ng for the entire procedure (sampling, filtration, storage and chemical separation). The $^{87}Sr/^{86}Sr$ ratios were normalized to a $^{86}Sr/^{88}Sr$ ratio of 0.1194. The reproducibility of $^{87}Sr/^{86}Sr$ ratio measurement was tested by replicate analysis of the NBS 987 standard with the mean value obtained during this study being 0.710236 ± 0.000024 (2σ, n = 13).

[13] δ^2H and $\delta^{18}O$ values (‰ vs. VSMOW) were determined on a Finnigan MAT 252 mass spectrometer following the gas-water equilibration technique of *Epstein and Mayeda* [1953] and *Oshumi and Fujini* [1986]. All samples were analyzed in duplicates. Analytical uncertainty, based on replicate analyses of international and laboratory standards, are ±0.8‰ for δ^2H and ±0.1‰ for $\delta^{18}O$. The isotopic composition of sulfur is expressed as $\delta^{34}S_{SO4}$ with respect to the CDT standard. The $\delta^{34}S_{SO4}$ was measured on SO_2 obtained from CdS precipitated after reduction of the dissolved sulfate. Analytical uncertainty for $\delta^{34}S_{SO4}$, based on replicate analyses of international and laboratory standards, is 0.3‰.

4. Results

[14] The chemical and oxygen, deuterium, boron, sulfur, and strontium isotopic results of the investigated groundwater are summarized in Tables 1 and 2. The results of the loess leaching experiments are reported in Table 3. Figures 5–8 illustrate the chemical composition, stable isotopes of oxygen-deuterium, strontium isotopes, and boron isotopes results, respectively.

[15] The chemical results enable us to discriminate between different water types: Na-Mg-Cl water type characterizes the saline groundwater in the Avedat (Eocene) aquitard, and groundwater in the shallow alluvial aquifer along Nahal Besor (Wadi Gaza) with typical Na/Cl ratios between 0.86 and 1 and Br/Cl ratios of $<1.5 \times 10^{-3}$ (marine ratio). Na-HCO_3-SO_4-Cl water type characterizes the saline groundwater in the central part of the aquifer (Israel) and the eastern part of the Gaza Strip, with typical high Na/Cl (>1), and marine Br/Cl ($\sim 1.5 \times 10^{-3}$) ratios. Ca-chloride water type characterizes the saline groundwater in the western part of the aquifer near the seashore with typical low Na/Cl (<0.86) and marine Br/Cl ($\sim 1.5 \times 10^3$) ratios.

4.1. Avedat Group Aquitard and Shallow Alluvial Aquifer Along Nahal Besor (Wadi Gaza)

[16] Groundwater from the Avedat (Eocene) aquitard is characterized by relatively high salinity (TDS up to 5 g/L),

Table 1. Chemical Data of Groundwater From the Southern Coastal Aquifer and Gaza Strip

Well Name	Date[a]	Ca, mg/L	Mg, mg/L	Na, mg/L	K, mg/L	Cl, mg/L	SO_4, mg/L	HCO_3, mg/L	NO_3, mg/L	Br, mg/L	B, mg/L	Sr, mg/L	TDS, mg/L
Avedat Group Aquitard													
Ein Aqev	9/14/98	168	95	644	9.8	1137	393	366	0.8	2.4	0.8	6.8	2823
Haluza well	9/14/98	257	173	1296	20	2423	528	173	30	6.0	-	-	4906
Haluza well	4/20/90	188	108	932	19	1735	442	195	11	7.5	-	-	3630
BSO3	8/9/90	290	126	1740	26	3150	800	245	10	9	-	-	6180
RH25	3/10/97	350	255	2000	27	3589	1042	245	-	9.4	-	-	7518
Beer Osnat	4/7/87	266	155	1114	15	2073	618	283	-	-	-	-	4521
T-24 (Figure 4)	2/19/95	98	57	256	4	496	114	307	20	2	-	-	1351
T-22 (Figure 4)	2/19/95	122	56	274	3	492	134	220	10	2	-	-	1310
T-22 (Figure 4)	7/26/94	102	53	261	2	495	86	302	11	-	-	-	1311
Shallow Alluvial Aquifer													
Nakaz Nirim 1	7/7/99	123	60	367	8.6	643	242	298	13.1	10.4	0.5	2.5	1767
Nakaz Nirim 1	8/16/01	129	62	343	9.1	618	208	386	13.5	8.7	0.5	2.7	1781
Nakaz Nirim 2	8/16/01	119	69	445	8.6	715	279	265	11.5	10.5	0.7	3.4	1926
Nakaz Nirim 3	8/16/01	115	59	338	7.6	587	199	277	12.9	10.3	0.5	2.8	1608
Nakaz Gevulot	8/16/01	182	83	350	9.0	800	216	259	9.4	24.1	0.5	5.0	1938
Rubia 5/7	8/16/01	83	49	661	14	921	171	406	0.1	2.5	1.3	2.5	2312
Urim 6/8 Amra	8/16/01	180	117	1196	32	1641	599	619	0.2	8.7	1.7	6.1	4401
Nakaz Holit Reim	10/9/01	264	165	1109	17	2077	616	346	0.8	15	1.4	7.1	4618
Central North													
Kfar Aza 1	7/7/99	36	53	910	7.4	1037	278	548	33	3.0	2.3	1.3	2911
Kfar Aza 2	7/7/99	39	61	1048	9.6	1247	477	494	32	3.5	3.0	1.6	3417
Nahal Oz 2	7/14/99	29	48	1017	8.3	1156	373	475	198	3.3	3.1	1.2	3312
Nir Am 13	9/7/99	31	41	432	5.0	483	133	461	20	1.3	1.3	1.1	1609
Nahal Oz 1	7/7/99	26	47	1056	7.8	1193	365	585	66	3.4	3.2	1.2	3354
Nahal Oz 2	8/24/99	33	68	1088	9.8	1367	532	455	35	3.9	3.2	1.6	3598
Kefar Aza 2	8/16/01	41	64	1018	10.2	1241	416	500	26	3.5	3.5	1.8	3324
Nir Am 13	9/5/01	34	44	458	5.2	502	152	476	17	1.4	1.5	1.2	1692
Nir Am 10	9/5/01	27	31	277	3.5	276	69	389	26	1.0	0.9	0.8	1100
Nir Am 14A	9/5/01	33	34	252	4.0	293	62	329	25	1.2	0.7	0.9	1035
Nir Am 17A	9/5/01	44	34	240	5.0	286	58	363	23	1.0	0.7	0.8	1054
Shokeda 6	6/2/99	41	60	843	7.7	1049	422	445	20	3.0	2.7	1.5	2895
Shoqeda 6	9/10/01	41	59	881	7.4	1072	376	434	16	2.5	2.9	1.6	2894
Alumim 2	9/5/01	98	152	1354	12	1851	694	336	16	4.5	2.1	4.1	4524
Central South													
Moshavei Negev 2	6/25/98	97	80	955	12	1356	626	211	24	3.6	1.4	3.1	3370
Nirim 2	8/23/99	92	67	501	8.2	822	326	148	14	11	0.6	3.0	1993
Moshavei Negev 2	8/17/99	90	80	1135	14	1406	644	187	26	3.8	1.3	2.8	3590
Re'im 1	6/24/98	59	52	460	8.4	611	235	244	32	1.7	0.8	1.7	1706
Nirim 2	7/7/99	101	68	540	8.6	817	313	168	14	11	0.8	2.9	2044
Khesufim 2	8/17/99	91	78	964	11	1360	1643		24	3.4	1.9	2.8	4179
Nirim 5	6/1/98	68	64	1009	12	1256	784	195	29	3.4	2.2	2.2	3425
Moshaviei hanegev 2	11/6/01	95	87	926	13	1359	537	232	21	3.2	1.5	3.0	3276
Nirim 2 saline	11/6/01	26	27	586	6.8	562	343	303	25	2.1	2.1	1.9	1885
Nirim 4	10/18/01	41	43	728	7.0	795	507	242	34	3.5	2.0	1.4	2404
Nirim 5	11/6/01	66	60	980	10.5	1172	674	217	23	3.2	2.3	2.2	3208
Shoqeda 2	9/5/01	92	147	1120	10.6	1653	734	329	16	4.1	2.1	4.3	4113
Reim 1	9/10/01	69	57	463	7.4	692	239	248	37	2.5	0.8	2.0	1818
Reim 1		69	56	449	7.8	696	214	255	35	2.7	0.9	2.4	1788
Gaza Strip													
A/123 - Mohamed Deeb taha	5/26/01	78	29	43	1.2	79.2	40	231	107	1.0	0.1	0.7	612
A/159 - Shaban Abu Asser	5/26/01	465	90	708	9.8	1924	165	172	140	6.7	0.1	7.6	3688
E/158 - Kamel Shath	5/26/01	277	53	183	18	546	204	165	395	2.6	0.1	3.6	1849
R/162G - Gaza Municipality	5/26/01	91	70	321	13	538	153	366	139	1.3	0.6	2.6	1696
C/36 - Mohamed Mustafa Khalil	5/26/01	56	54	544	3.6	759	98	480	108	2.3	1.4	1.5	2108
1-G-2 - Waheb El Wadia	5/26/01	27	40	641	5.3	764	128	514	40	2.7	1.6	0.9	2163
R/112 - Gaza Municipality	5/26/01	75	52	399	16	613	129	380	107	1.6	1.0	2.6	1778
R/108 - Ismail Shmalakh	5/26/01	70	55	305	4.2	472	182	218	147	1.3	0.6	2.3	1458
R/189 - Saleh El Jadba	5/27/01	139	78	414	34	551	235	441	398	1.4	0.7	2.0	2295
E/63 - Old Fighters	5/27/01	433	86	480	7.0	1442	162	151	149	4.4	0.1	9.9	2927
G/13 - Mahmoud Abu Areban	5/28/01	124	162	745	7.7	1095	431	357	286	2.8	0.8	8.8	3221
G/26 - Hamed Abu Maluh	5/28/01	128	106	662	10	992	402	394	183	2.7	0.9	6.6	2889
F/156 - Mohamed Galayny	5/28/01	127	90	422	4.9	857	263	213	61	2.1	0.7	3.1	2044
1-G-1 - Jamal Abu Dayia	5/28/01	105	85	199	2.5	413	66	405	156	1.1	0.4	4.6	1438
1-B-1 - Hamed El Debri	5/28/01	86	65	502	7.2	811	271	249	55	2.0	1.0	2.5	2053
J-32 in	11/20/01	113	116	781	27	1150	439	432	211	3.8	1.8	6.5	3280
Q-57 - Mustafa Khalia El Astal	11/20/01	46	49	467	5.1	553	119	535	53	2.5	1.1	1.1	1830
C/43 - Ahmed mohamed Hamadan	11/20/01	73	59	541	4.0	771	133	461	166	-	2.1	1.7	2213
R/189 - Saleh El Jadba	11/20/01	161	82	444	28	556	234	497	389	1.2	0.9	2.4	2396
G/26 - Hamed Abu Maluh	11/20/01	154	126	649	10	1049	401	406	175	2.6	1.0	8.3	2982

Table 1. (continued)

Well Name	Date[a]	Ca, mg/L	Mg, mg/L	Na, mg/L	K, mg/L	Cl, mg/L	SO_4, mg/L	HCO_3, mg/L	NO_3, mg/L	Br, mg/L	B, mg/L	Sr, mg/L	TDS, mg/L
R/112 - Gaza Municipality	11/20/01	94	63	435	16	718	153	388	106	1.9	1.1	3.2	1980
H/97 - Mohamed El Falit	11/20/01	141	99	622	9.7	964	363	352	219	2.6	0.9	7.4	2781
1-G-2 - Waheb El Wadia	11/20/01	25	37	637	5.3	749	151	517	38	2.5	1.6	1.0	2164
R/254 - Gaza Municipality	11/20/01	48	36	340	5.8	389	126	413	52	1.1	1.1	1.7	1414
S/72 - Briaj Municipality	11/20/01	91	81	643	9.3	1006	360	240	54	2.4	1.2	3.0	2491
1-B-1 - Hamed El Debri	11/20/01	95	77	519	8.0	878	282	262	71	2.2	1.4	3.0	2198
J/92 - Mohamed Hassan Abu Jaber	11/20/01	99	115	473	7.3	783	209	435	262	4.2	1.2	5.7	2394
R/190 - Ibrahim Al Issy	11/20/01	163	76	368	7.5	446	217	459	459	1.0	0.6	3.1	2200
Erez 2A	9/5/01	50	40	148	25.1	198	30.3	338	38	0.7	0.4	1.1	869
Nakaz South NADAR 7	10/18/01	28	22	64	5.7	47	111.6	163	7.1	9.8	0.2	1.6	460
Netzarim 3	10/18/01	76	52	237	4.0	313	31.2	449	82	1.4	0.4	2.7	1250
Netzarim 1	10/18/01	90	57.6	254	5.8	393	39.6	520	68	0.9	0.5	3.7	1434

[a]Read 9/14/98 as 14 September 1998.

Na-Mg-Cl composition, marine and lower ($<1.5 \times 10^{-3}$) Br/Cl ratios, and marine $\delta^{11}B$ values (~40‰; Table 1). Groundwater from the shallow alluvial aquifer exhibits two different water components (Figure 9): (1) saline end-member with chemical features identical to that of groundwater from the Avedat aquitard (e.g., Na/Cl ~ 0.86, low Br/Cl, low $^{87}Sr/^{86}Sr$ ratios, and $\delta^{11}B \sim 40‰$); and (2) fresh end-member with conspicuous high Br/Cl ratio ($\gg 1.5 \times 10^{-3}$), high $^{87}Sr/^{86}Sr$, $\delta^{11}B \sim 35‰$; and low $\delta^{18}O$ values.

4.2. Saline Groundwater in the Central Part of the Coastal Aquifer

[17] Groundwater from the central part of the coastal aquifer has a salinity range (as TDS) of 1 to 4 g/L. The $\delta^{18}O$-$\delta^{2}H$ relationships (Figure 6) in the Na-rich groundwater exhibit a slope of 5.6 that is identical to the slope measured in groundwater from the Avedat Group aquitard and local precipitation in the recharge area in northern Negev [*Nativ and Nissim*, 1992; *Nativ et al.*, 1995; *Adar and Nativ*, 2003]. The groundwater is characterized by Na-HCO_3-Cl composition in the northern part of the research area and Na-SO_4-Cl type in the southern area. In both areas the groundwater has conspicuously high Na/Cl (>1), marine Br/Cl (1.5×10^{-3}), high B/Cl, and low Ca/Cl ratios (Figure 10). In the southern part of the research area (south from Nahal Besor, Figure 1a) the SO_4/Cl ratios are high whereas in the northern section the HCO_3/Cl ratios are high relative to those in the Avedat aquitard. The Na/Cl ratios are negatively and positively correlated with Ca/Cl and B/Cl ratios, respectively (Figure 10). The $^{87}Sr/^{86}Sr$ ratios show an inverse correlation with elemental Sr (Figure 7). The $\delta^{34}S_{SO4}$ value of the Na-rich groundwater is about 13‰. This value is slightly lower than the $\delta^{34}S_{SO4}$ values (15‰) reported in secondary gypsum veins in fractures intersecting the chalk [*Issar et al.*, 1988] and higher than that of uncontaminated groundwater of the Avedat Group aquitard in Ramat Hovav area (10.8‰) [*Adar and Nativ*, 2003]. The Na-rich saline groundwater in the central part of the southern coastal aquifer is characterized by high boron content and high B/Cl ratios (i.e., 0.012 relative to 8×10^{-4} in seawater; Table 1). The boron isotopic ratios (Figure 8) reflect mixing between two sources: (1) saline groundwater with high $\delta^{11}B$ values (~48‰); and (2) fresh groundwater with low $\delta^{11}B$ values (~25‰; Figure 8). Relatively low $\delta^{11}B$ values (20–30‰) were found in low-saline groundwater elsewhere in the Mediterranean coastal aquifer, reflecting leaching of the aquifer matrix during the recharge process [*Vengosh et al.*, 1994, 1999].

4.3. Groundwater in the Gaza Strip

[18] The chemical data of groundwater in the Gaza Strip reveal three types of groundwater. The first is groundwater with high Na/Cl ratios that mimic the composition of the Na-rich groundwater in the central section of the aquifer. In most cases, the high Na/Cl signature is found in wells located along the eastern part of the Gaza Strip that is downgradient from the central saline Na-rich groundwater. The second is saline groundwater in the western part of the aquifer along the seashore that is characterized by a Ca-chloride composition with low Na/Cl (<0.86), B/Cl ($<8 \times 10^{-4}$), SO_4/Cl (<0.05) ratios, marine (1.5×10^{-3}) Br/Cl ratios, and marine $\delta^{11}B$ values (~39‰). Similar composition was found in saline groundwater associated with seawater intrusion in the Mediterranean coastal aquifer [*Vengosh et al.*, 1994; *Yechieli et al.*, 2001] and elsewhere [e.g., *Jones et al.*, 1999]. The third is groundwater with high nitrate content (up to 450 mg/L). The nitrate contents are positively correlated with Ca^{2+}, Mg^{2+}, and $^{87}Sr/^{86}Sr$ ratios (Figure 11).

4.4. Leaching of the Loess Soil

[19] The loess leaching results (Table 3) show wide ranges of salinity and water chemistry. Effluents with low salt content are characterized by extremely high Na/Cl ($\gg 1$) whereas saline extractions have lower Na/Cl ratios ~1. The Na/Cl ratios measured in loess extraction are positively correlated with Ca/Cl and B/Cl ratios (Figure 12). Excess of Na^+ over Cl^- was reported also in previous leaching experiments of loess soil in the Negev [*Dan and Yaalon*, 1982]. We, moreover, found that the saline effluents have low Br/Cl ratio ($<1.5 \times 10^{-3}$), indicating that the salinity is derived primarily from dissolution of halite in the loess soil (Figure 12). The water extraction of the loess soil yields $^{87}Sr/^{86}Sr$ ratios of 0.708207 to 0.708330, which are higher that those measured in the underlying groundwater. Loess extraction yields high B/Cl (1.8×10^{-3} to 1.5×10^{-2}) and $\delta^{11}B$ values in the range of 16.7‰ to 31‰

Table 2. Isotopic Data of Groundwater from the Southern Coastal Aquifer and Gaza Strip

Well Name	Date	$\delta^{11}B$, ‰	$^{87}Sr/^{86}Sr$	$\delta^{18}O$, ‰	$\delta^{2}H$, ‰	$\delta^{34}S$, ‰
		Avedat Group Aquitard				
Ein Aqev	9/14/98	45.0 ± 2	-	-	-	-
Shallow alluvial aquifer						
Nakaz Nirim 1	7/7/99	35.8 ± 0.2	0.708105 ± 0.00001	-	-	-
Nakaz Nirim 1	8/16/01	38.2 ± 0.1	0.708107 ± 0.000009	−5.1	−21.0	12.5
Nakaz Nirim 2	8/16/01	39.5 ± 0.2	0.708058 ± 0.000008	−5.0	−21.8	-
Nakaz Nirim 3	8/16/01	38.4 ± 0.1	0.708107 ± 0.000011	−5.2	−22.3	-
Nakaz Gevulot	8/16/01	38.9 ± 0.1	0.708031 ± 0.000011	−5.5	−24.6	-
Rubia 5/7	8/16/01	37.1 ± 0.1	0.708037 ± 0.000012	−4.9	−21.5	-
Urim 6/8 Amra	8/16/01	44.1 ± 0.1	0.707985 ± 0.000009	−3.8	−17.0	-
Nakaz Holit Reim	9/10/01	40.8 ± 0.2	0.707973 ± 0.000009	−4.5	−21.0	-
		Central North				
Kfar Aza 1	7/7/99	42.9 ± 0.1	0.708178 ± 0.000007	-	-	-
Kfar Aza 2	7/7/99	46.2 ± 0.1	0.708160 ± 0.000009	-	-	-
Nahal Oz 2	7/14/99	45.7 ± 0.1	0.708151 ± 0.000007	-	-	-
Nir Am 13	9/7/99	34.8 ± 0.1	0.708139 ± 0.000009	−4.3	−26.9	-
Nahal Oz 1	7/7/99	45.6 ± 0.1	0.708137 ± 0.000009	-	-	-
Nahal Oz 2	8/24/99	47.2 ± 0.1	0.708186 ± 0.000009	-	-	-
Kefar Aza 2 (salty)	8/16/01	45.8 ± 0.1	0.708160 ± 0.000009	−4.2	−17.8	13.5
Nir Am 13	9/5/01	36.6 ± 0.1	0.708158 ± 0.000008	−4.4	−17.7	-
Nir Am 10	9/5/01	28.8 ± 0.1	0.708183 ± 0.000009	−4.1	−15.9	-
Nir Am 14A	9/5/01	26.0 ± 0.1	0.708161 ± 0.000009	−3.5	−13.7	-
Nir Am 17A	9/5/01	28.6 ± 0.1	0.708026 ± 0.00001	−4.0	−15.4	-
Shokeda 6	6/2/99	46.5 ± 0.1	0.708130 ± 0.00001	-	-	-
Shoqeda 6	9/10/01	46.2 ± 0.2	0.708096 ± 0.000009	−4.4	−18.6	-
Alumim 2	9/5/01	47.4 ± 0.1	0.708074 ± 0.000008	−4.4	−18.7	13.1
		Central South				
Moshavei Negev 2	6/25/98	-	-	-	-	-
Nirim 2	8/23/99	-	-	-	-	-
Moshavei Negev 2	8/17/99	39.4 ± 0.1	0.708097 ± 0.000008	-	-	-
Re'im 1	6/24/98	-	-	-	-	-
Nirim 2	7/7/99	-	-	-	-	-
Khesufim 2	8/17/99	43.8 ± 0.1	0.708113 ± 0.000008	-	-	-
Nirim 5	6/1/98	-	-	-	-	13.0
Moshaviei hanegev 2	11/6/01	40.3 ± 0.1	0.708078 ± 0.000008	−4.6	−19.7	-
Nirim 2 saline	11/6/01	46.0 ± 0.1	0.708070 ± 0.000008	−4.9	−20.1	-
Nirim 4	10/18/01	43.3 ± 0.1	0.708096 ± 0.000008	−4.9	−21.4	-
Nirim 5	11/6/01	45.3 ± 0.1	0.708109 ± 0.000008	−4.6	−20.4	-
Shoqeda 2	9/5/01	47.4 ± 0.1	0.708027 ± 0.00001	−4.3	−18.3	-
Reim 1	9/10/01	38.1 ± 0.1	0.708158 ± 0.00001	−4.8	−20.7	-
Reim 1	11/6/01	38.1 ± 0.1	0.708134 ± 0.00001	−4.9	−18.4	-
		Gaza Strip				
A/123 - Mohamed Deeb taha	5/26/01	27.2 ± 0.2	0.708183 ± 0.000009	−4.5	−16.4	-
A/159 - Shaban Abu Asser	5/26/01	48.6 ± 0.1	0.708965 ± 0.00001	−4.1	−14.9	-
E/158 - Kamel Shath	5/26/01	42.0 ± 0.1	0.708158 ± 0.00001	−4.6	−19.2	-
R/162G - Gaza Municipality	5/26/01	17.2 ± 0.1	0.708399 ± 0.00001	−4.4	−16.8	-
C/36 - Mohamed Mustafa Khalil	5/26/01	-	0.708980 ± 0.000009	−4.1	−15.6	-
1-G-2 - Waheb El Wadia	5/26/01	-	0.709001 ± 0.000009	−4.1	−14.9	-
R/112 - Gaza Municipality	5/26/01	34.4 ± 0.2	0.708354 ± 0.000008	−4.5	−17.8	-
R/108 - Ismail Shmalakh	5/26/01	39.9 ± 0.1	0.708733 ± 0.000009	−4.5	−16.4	-
R/189 - Saleh El Jadba	5/27/01	37.0 ± 0.1	0.708692 ± 0.000009	−4.5	−17.3	-
E/63 - Old Fighters	5/27/01	46.3 ± 0.1	0.708570 ± 0.00001	−4.2	−16.1	-
G/13 - Mahmoud Abu Areban	5/28/01	30.3 ± 0.1	0.708430 ± 0.00001	−4.4	−17.2	-
G/26 - Hamed Abu Maluh	5/28/01	38.9 ± 0.1	0.708708 ± 0.00001	−4.5	−18.0	-
F/156 - Mohamed Galayny	5/28/01	42.0 ± 0.1	0.708674 ± 0.000009	−4.6	−17.6	-
1-G-1 - Jamal Abu Dayia	5/28/01	37.0 ± 0.1	0.708518 ± 0.000009	−4.4	−16.1	-
1-B-1 - Hamed El Debri	5/28/01	38.8 ± 0.2	0.708404 ± 0.000011	−4.2	−15.8	-
J-32 in	11/20/01	38.0 ± 0.1	0.708593 ± 0.000008	-	-	-
Q-57 - Mustafa Khalia El Astal	11/20/01	27.8 ± 0.1	0.708194 ± 0.000007	-	-	-
C/43 - Ahmed mohamed Hamadan	11/20/01	45.3 ± 0.1	0.708380 ± 0.000008	-	-	-
R/189 - Saleh El Jadba	11/20/01	36.0 ± 0.1	0.708385 ± 0.000008	-	-	-
G/26 - Hamed Abu Maluh	11/20/01	35.9 ± 0.1	0.708675 ± 0.000007	-	-	-
R/112 - Gaza Municipality	11/20/01	41.5 ± 0.1	0.708633 ± 0.000007	-	-	-
H/97 - Mohamed El Falit	11/20/01	37.2 ± 0.2	0.708613 ± 0.000007	-	-	-
1-G-2 - Waheb El Wadia	11/20/01	33.1 ± 0.2	0.708150 ± 0.000009	-	-	-
R/254 - Gaza Municipality	11/20/01	43.4 ± 0.2	0.708548 ± 0.000008	-	-	-
S/72 - Briaj Municipality	11/20/01	38.6 ± 0.1	0.708158 ± 0.000009	-	-	-
1-B-1 - Hamed El Debri	11/20/01	48.6 ± 0.1	0.708165 ± 0.000009	-	-	-
J/92 - Mohamed Hassan Abu Jaber	11/20/01	16.9 ± 0.1	0.708463 ± 0.000009	-	-	-
R/190 - Ibrahim Al Issy	11/20/01	44.2 ± 0.1	0.708491 ± 0.000009	-	-	-

Table 2. (continued)

Well Name	Date	$\delta^{11}B$, ‰	$^{87}Sr/^{86}Sr$	$\delta^{18}O$, ‰	$\delta^{2}H$, ‰	$\delta^{34}S$, ‰
Erez 2A	9/5/01	21.6 ± 0.1	0.708294 ± 0.00001	−4.7	−18.8	-
Nakaz South NADAR 7	10/18/01	23.7 ± 0.1	0.708607 ± 0.00001	−4.0	−14.2	-
Netzarim 3	10/18/01	38.9 ± 0.1	0.708472 ± 0.000008	−3.8	−13.6	-
Netzarim 1	10/18/01	39.3 ± 0.1	0.708576 ± 0.00001	−3.8	−14.1	-

that are lower than those of the underlying saline groundwater (48‰).

5. Discussion

5.1. Origin of Groundwater in the Shallow Alluvial Aquifer

[20] The shallow alluvial aquifer along Nahal Besor (Wadi Gaza) overlies the regional Avedat Group aquitard. Given the relatively high potentiometric level of the Avedat aquitard and the direct hydrogeological contact (Figure 3), the regional groundwater flows to the shallow aquifer. The chemical composition of the shallow groundwater from the alluvial aquifer (Figure 9) reflects two distinctive sources: (1) a saline source with chemical and isotopic compositions that are similar to those of groundwater from the Avedat Group aquitard, and (2) a freshwater source enriched in Br- that is derived from anthropogenic contamination. For example, the low $^{87}Sr/^{86}Sr$ ratio observed in the shallow groundwater (>0.70795; Figure 9) is consistent with the Eocene marine isotopic signal of the Avedat Group aquitard. Likewise, the $\delta^{11}B$ (∼40‰; Figure 8) values are also similar to that of saline springs that emerge from the Avedat Group aquitard (Rosenberg, personal communication). In contrast, the $\delta^{18}O$ and $\delta^{2}H$ values of the low-saline groundwater are low and are consistent with the depleted values measured in floodwater in the mountain region of the central Negev [*Magaritz et al.*, 1984]. In addition, the shallow groundwater is characterized by conspicuous high Br/Cl ratio ($\gg 1.5 \times 10^{-3}$; Figure 9) that is different from that in Avedat aquitard ($\sim 1 \times 10^{-3}$).

[21] We attribute the high Br/Cl and low $\delta^{18}O$ signatures to the lateral discharge of Br-rich floodwater into the alluvial aquifer. We suggest that the high bromide originated from industrial effluents that were historically discharged from the Ramat Hovav industrial park [*Adar and Nativ*, 2003; *Nativ and Adar*, 1997] and were transported during flood events. High Br level is indeed found in current floodwaters despite the fact that active discharge of wastewater has ceased more than a decade ago [*Keshet*, 1992, 1999]. Consequently, the relationship between Br/Cl and $\delta^{18}O$ values (Figure 9) suggests mixing between the saline groundwater from the Avedat Group aquitard (low Br/Cl and high $\delta^{18}O$) and floodwater (high Br/Cl and low $\delta^{18}O$). The recharge of human-induced high Br/Cl water into the alluvial aquifer has important implications for the risks of contamination of the regional coastal aquifer, which is in hydraulic continuity with the shallow alluvial aquifer in the northwestern section of Wadi Gaza (Figures 1b and 4). Hence, in the southern coastal aquifer the Br/Cl is a good monitoring tool to trace the progressive mixing of pristine (yet saline) waters ($<1 \times 10^{-3}$) with floodwaters characterized by anthropogenic signature ($>1.5 \times 10^{-3}$).

5.2. Origin of the Na- and B-Rich Saline Groundwater

[22] The hydrogeological, hydrological, and geochemical data (Table 1 and Figures 1b and 3) clearly indicate that the saline groundwater from the Avedat aquitard flows into the eastern part of the coastal aquifer [*Nativ and Nissim*, 1992; *Livshitz*, 1999]. Yet the chemical composition of saline groundwater in the central part of the aquifer is entirely different from that of groundwater in Avedat aquitard. Saline groundwaters in the northern and southern parts of the research area have respectively Na-HCO_3-Cl and Na-SO_4-Cl compositions with Na/Cl > 1, while the saline groundwater in Avedat aquitard has a Na-Mg-Cl composition with Na/Cl < 1 (Table 1 and Figure 5). In contrast, the slope of $\delta^{18}O$ versus $\delta^{2}H$ values (5.6; Figure 6) is identical to that of the Avedat Group aquitard and local precipitation in the northern Negev [*Nativ and Nissim*, 1992; *Nativ et al.*, 1995; *Adar and Nativ*, 2003], thus indicating that most of the *water* is indeed derived from the Avedat aquitard.

[23] Typically, the Na-HCO_3 composition in coastal aquifers reflects displacement of seawater by fresh water (i.e., freshening). In this process sequential elution of seawater cations that are bond to exchangeable sites on clay minerals results in chromatographic enrichments of Mg^{2+}, K^{+}, and Na^{+} along flow paths [*Appelo*, 1994]. We use this analogy to suggest that the Na-rich groundwater is

Table 3. Results of Isotopic and Chemical Data of Solutions Extracted From Loess Soils Over the Coastal Aquifer

Site	$\delta^{11}B$, ‰	$^{87}Sr/^{86}Sr$	Ca, mg/L	Mg, mg/L	Na, mg/L	K, mg/L	Cl, mg/L	SO_4, mg/L	Br, mg/L	B, mg/L	Sr, mg/L	TDS, mg/L
Maagar Nahal Oz	23.4	0.708207	17	6.7	137	1.8	97	34	-	1.06	0.32	207
Baba Sali	17.5	0.708295	36	38	566	5.4	544	639	0.88	1.34	1.79	1832
Baba Sali	16.7	0.708307	78	57	850	25	1404	282	3.09	2.63	3.36	2704
Baba Sali	25.0	0.708330	40	26	654	8.8	934	263	3.51	4.20	1.77	1935
Nakaz Gevulot	31.0	0.708289	304	94	1602	15.8	3154	297	3.41	1.73	4.79	5476
Nakaz Gevulot	-	-	6.7	1.8	70	2.8	18	69	0.08	1.0	1.3	191
Shemorat Be'eri	-	-	9	5	51	1.9	7.5	7.8	-	0.22	0.16	93
Shemorat Be'eri	-	-	10	4	104	1.6	6.6	12	-	0.44	0.18	166
Shemorat Be'eri	-	-	11	5	40	2	18	13	-	0.17	0.22	1606

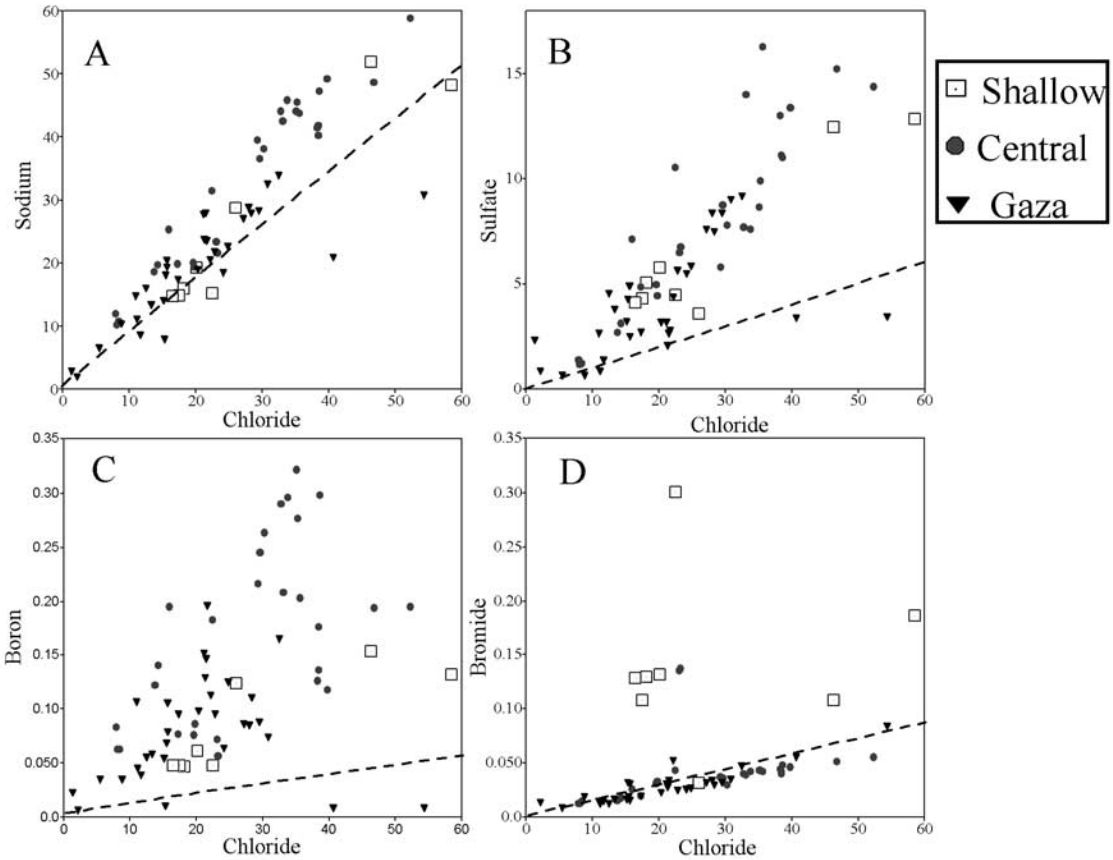

Figure 5. Sodium, sulfate, bromide, and boron versus chloride concentrations (in meq/L) of groundwater from the southern coastal aquifer. Note the distinction of the different water types: shallow groundwater (squares), central (solid circles), and Gaza Strip (triangles). The dashed lines represent dilution of seawater. Note the enrichment of Br over the marine ratio in the shallow groundwater and the relative enrichments of sodium, sulfate, and boron in most water types.

the central part of the aquifer was generated via reverse base exchange reactions:

$$1/2\ Ca^{2+} + Na\text{-}X \longleftrightarrow 1/2\ Ca\text{-}X + Na^{+} \qquad (1)$$

where Na-X and Ca-X represent the exchangeable cations on clay minerals.

[24] The Na-HCO_3 and Na-SO_4 compositions of the saline groundwater are completely different from the Ca-chloride saline plumes in the central part of the Mediterranean coastal aquifer [*Vengosh et al.*, 1999] that are about 50 km north of the research site. *Vengosh et al.* [1999] suggested that saline plumes are derived from up flow of pressurized saline groundwater. The basic foundation of their model was the chemical composition of the saline plumes that have a Ca-chloride composition with low Na/Cl ratios (<0.86) that resemble the composition of modified seawater. Hence we rule out the possibility that the Na-rich water in the southern aquifer is derived from deep underlying sources. Likewise, *Fink* [1970] identified hypersaline brines (TDS up to 115 g/L) in the deep subaquifer in Gaza Strip that potentially can be the source for salinization in the central part of the coastal aquifer. However, the chemical composition of these brines (e.g., Ca-chloride type, Na/Cl $\sim$ 0.86) is, again, different from the saline groundwater in the study area.

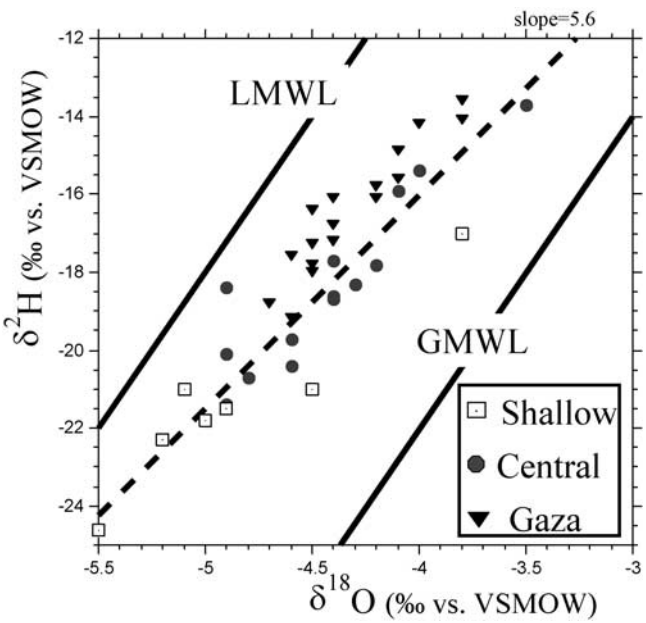

Figure 6. Plots showing δ^2H versus $\delta^{18}O$ values (versus SMOW) of groundwater from the coastal aquifer, divided by the different water types. Note the slope of the data point (5.6) relative to the local meteoric water line (LMWL) and global meteoric water line (GMWL).

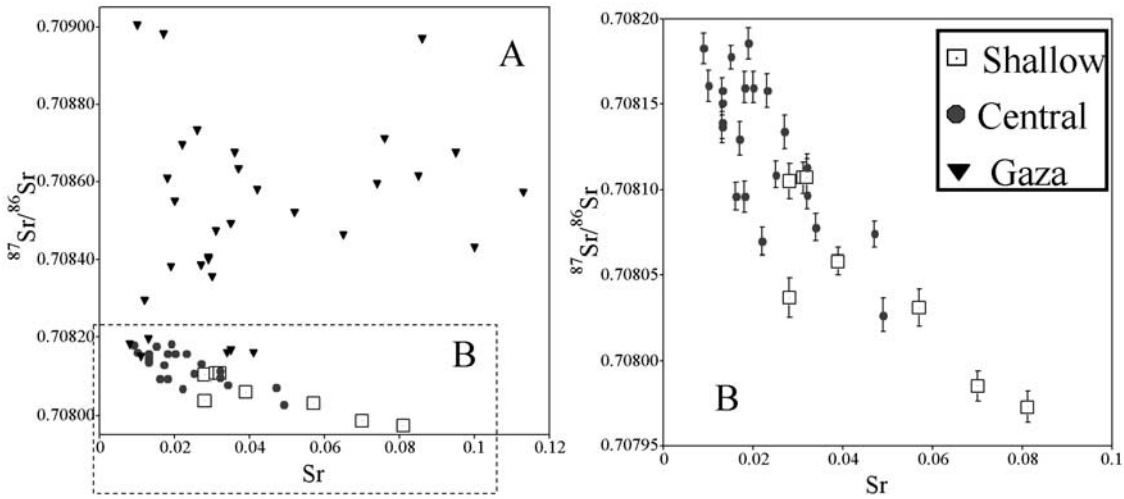

Figure 7. (a) Plot showing $^{87}Sr/^{86}Sr$ ratios versus strontium concentrations (in meq/L) of groundwater from the coastal aquifer, divided by the different water groups. Note the relatively narrow $^{87}Sr/^{86}Sr$ ratios measured in the central part of the aquifer relative the wide range in the Gaza Strip. (b) Plot showing $^{87}Sr/^{86}Sr$ ratios versus strontium concentrations (in meq/L) in only groundwater measured in the shallow and central groundwater. The positive correlation indicates mixing between Eocene saline groundwater with $^{87}Sr/^{86}Sr \sim 0.70795$ and a high $^{87}Sr/^{86}Sr$ source ($\sim$0.7082) that was also measured in loess soil.

[25] In contrast, we present several evidences that water-rock interactions in the overlying loess soil generated Ca-rich solutions that triggered the base exchange reactions. First, the $^{87}Sr/^{86}Sr$ ratios of the Na-rich groundwater exhibit an inverse correlation with elemental Sr^{2+} (Figure 7) indicating that the depletion of Sr^{2+} (and hence Ca^{2+}) was accompanied by isotopic change that resembles the $^{87}Sr/^{86}Sr$ ratios found in loess leachates. Second, the $\delta^{34}S_{SO4}$ value measured in the Na-rich groundwater (13‰) is slightly lower than $\delta^{34}S_{SO4}$ values (15‰), presumably derived from gypsum dissolution in loess soil in the Negev [*Issar et al.*, 1988], and higher than that of uncontaminated groundwater of the Avedat Group aquitard in Ramat Hovav area (10.8‰) [*Adar and Nativ*, 2003]. These relationships might indicate that the dissolved sulfate in the Na-rich groundwater is derived from a mixture composed from the original Avedat groundwater and sulfate derived from dissolution of gypsum in the overlying loess soil. The relatively low $\delta^{34}S_{SO4}$ values also rule out sulfate reduction processes in the aquifer. Third, the $\delta^{13}C$ values (range of -4‰ to -15‰; data are from *Magaritz et al.* [1984]) rule out any biogenic processes (e.g., organic breakdown) that might control the elevated dissolved bicarbonate in the Na-rich groundwater. In sum, $^{87}Sr/^{86}Sr$, $\delta^{34}S_{SO4}$, and $\delta^{13}C$ variations in the Na-rich groundwater indicate that the loess is the source for the Ca source that triggered the base exchange reactions.

[26] We consider two scenarios for the base exchange reactions. First, long-term flushing of the loess soil resulted in dissolution of pedogenic carbonate and gypsum minerals and formation of Ca-rich solutions. The interaction of the Ca-rich solutions with clay minerals saturated with Na^+ on the exchangeable matrix resulted in base exchange reaction and elution of Na^+ to the groundwater. In this scenario the base exchange reactions took place *within* the aquifer, as the exchangeable sites on clays minerals were saturated with Na^+ due to the flow of the saline groundwater from the Avedat aquitard.

[27] The second scenario considers base exchange reactions in the overlying loess layers. The distribution of ions along the loess deposits is a function of climatic changes

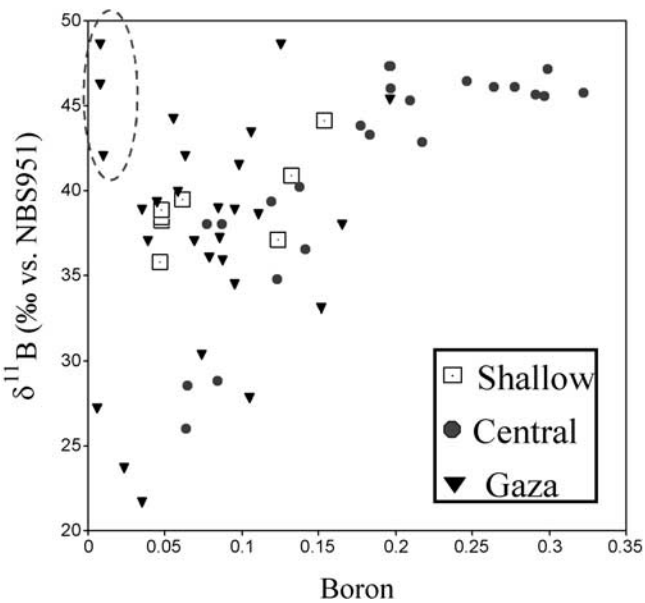

Figure 8. Values of $\delta^{11}B$ versus boron concentrations (in mmole/L) of groundwater from the coastal aquifer, which are divided by the different water groups. Note the correlation observed in groundwater from the central part of the aquifer relative the scatter distribution in the Gaza Strip. The dashed circle represents groundwater associated with seawater intrusion, characterized by high $\delta^{11}B$ and low B/Cl ratios.

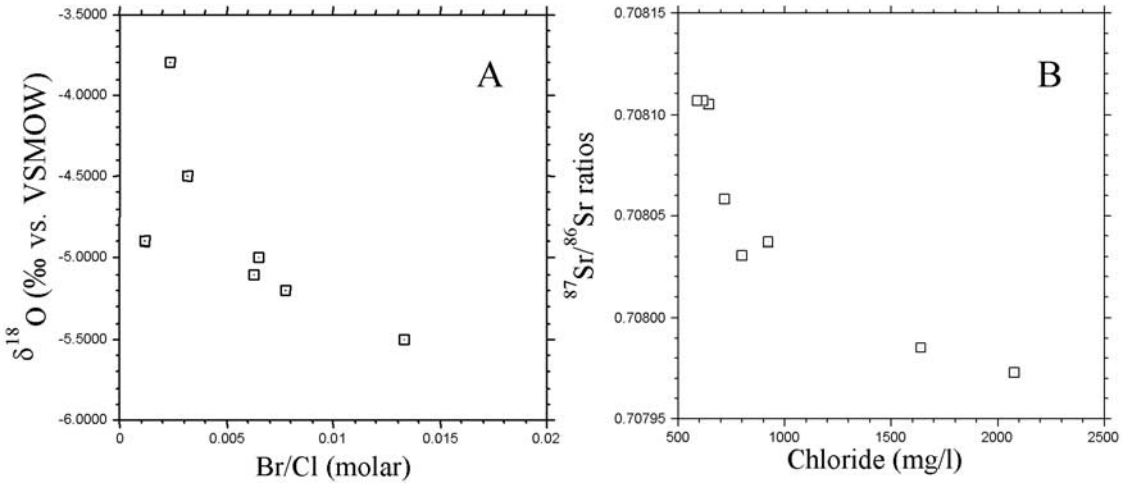

Figure 9. Chemical and isotopic variations in groundwater from the shallow alluvial aquifer: (a) $\delta^{18}O$ values versus Br/Cl (molar) ratios and (b) $^{87}Sr/^{86}Sr$ ratios versus chloride concentrations (mg/L). Note the mixing between saline groundwater having low $^{87}Sr/^{86}Sr$ ratios and Br/Cl ratios and high $\delta^{18}O$ with fresh water having high $^{87}Sr/^{86}Sr$ and Br/Cl and low $\delta^{18}O$ values.

during the Pleistocene. During arid periods, salts were accumulated in the soil whereas in humid phases the salts were flushed toward the lower section of the loess column and pedogenic carbonate horizon was formed [*Dan and Yaalon*, 1982; *Magaritz et al.*, 1988].

[28] In both scenarios we argue that the Ca-rich solutions were formed in the loess soil. *Dan and Yaalon* [1982] demonstrated that the loessial sequences in the Negev are predominantly composed of pedogenic carbonates (24 to 49%), while gypsum occurs only in the areas south of the 220 mm precipitation isohyet and increases with level of aridity. Water extraction of the loess soil as reported in the current (Table 3) and previous studies [*Dan and Yaalon*, 1982; *Magaritz et al.*, 1988] did not dissolve the carbonate phase as evidenced by the relatively low Ca^{2+} content that was measured in all these extraction experiments. However, it is assumed that under natural conditions and degradation of organic matter in the soil, acid conditions develop and the pedogenic carbonates are dissolved. Moreover, we argue that the formation of Ca-rich solution modified the chemical composition of the underlying groundwater, but the water contribution was insignificant, given the relatively low conductivity of the loess soil and the $\delta^{18}O$ and $\delta^{2}H$ values measured in the Na-rich groundwater (Figure 6).

[29] We attribute the distinction between Na-HCO_3 and Na-SO_4 composition in groundwater from the northern and southern areas to the composition of the overlying loess. In the northern part of the research area the source of the calcium could be the dissolution of calcium carbonate as inferred by the high bicarbonate concentration. In the southern part of the aquifer, sulfate is the predominant anion that balances the sodium enrichment, and therefore gypsum is a possible primary source for the Ca-rich solution. This interpretation is consistent with soil classification made by *Dan and Yaalon* [1982] that showed that saline and gypsiferous soils occur in the Negev only south

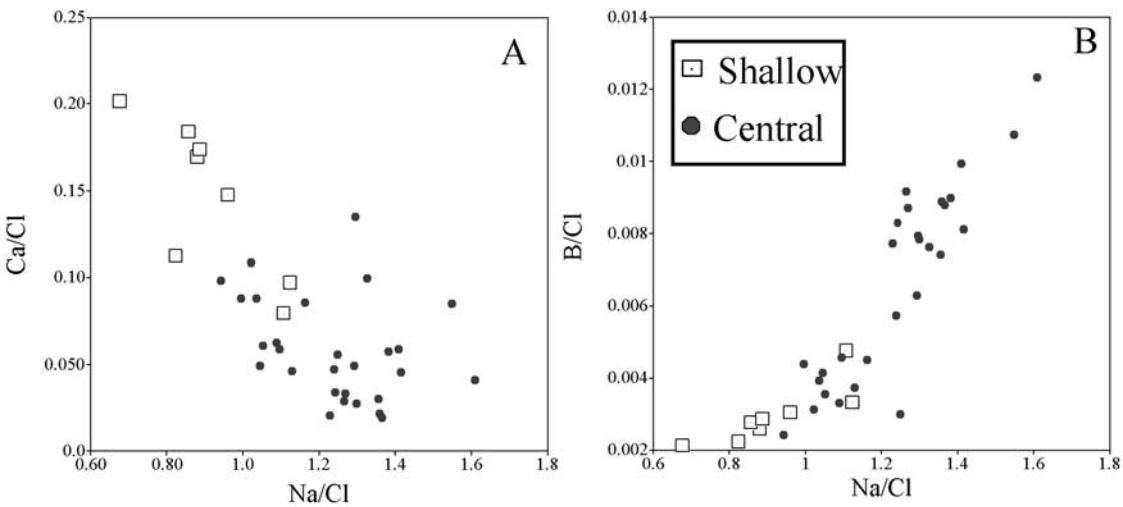

Figure 10. (a) Ca/Cl versus Na/Cl and (b) B/Cl versus Na/Cl (molar) ratios in groundwater. Note the respectively positive and negative relationships of Na/Cl with B/Cl and Ca/Cl ratios.

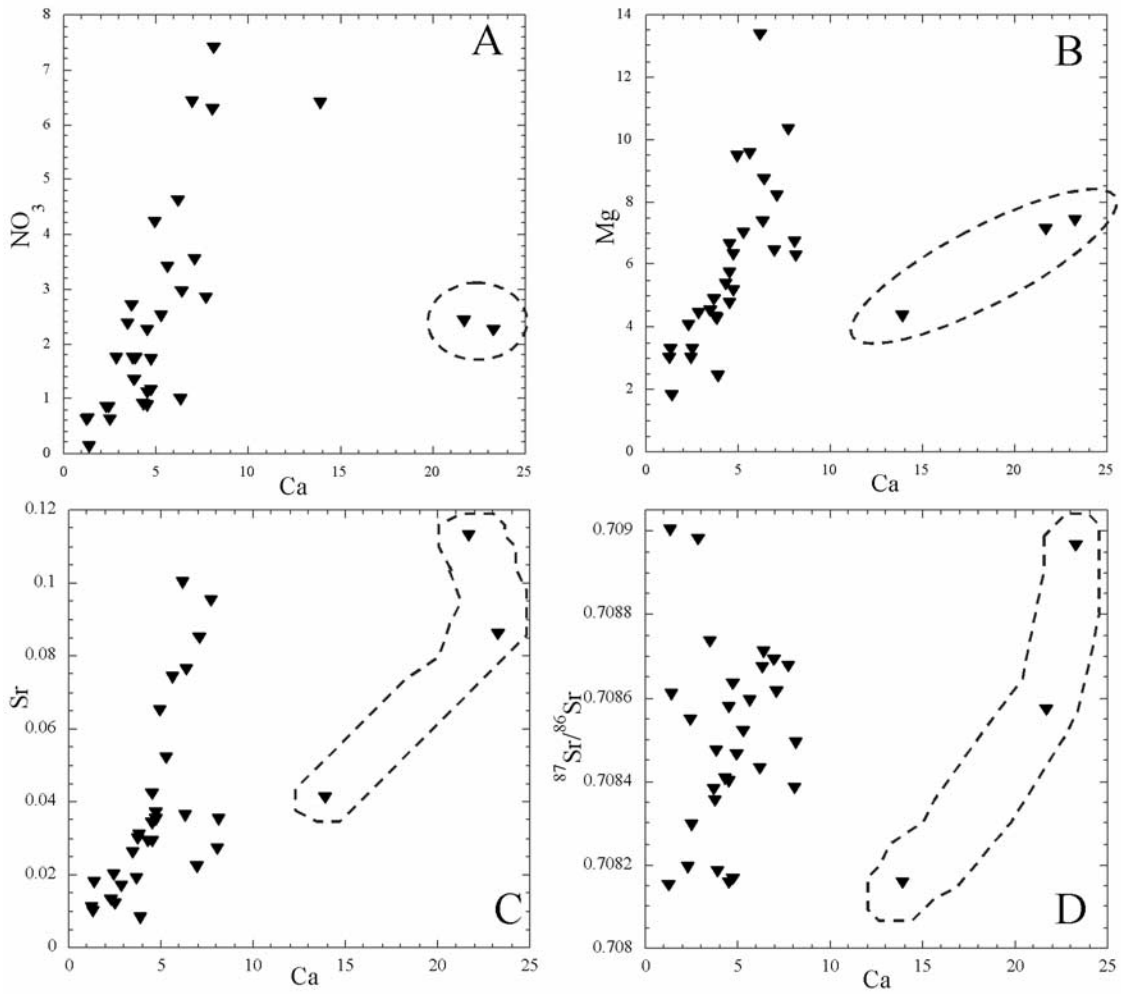

Figure 11. (a) Nitrate, (b) magnesium, (c) strontium, and (d) $^{87}Sr/^{86}Sr$ ratios versus calcium (meq/L) contents of groundwater from the Gaza Strip. Note the positive correlations observed in most groundwater samples. The dashed circles represent groundwater associated with seawater intrusion.

of the 220 mm precipitation isohyet. Moreover, they demonstrated that the depth of the calcium horizon also decreases with aridity. Likewise, *Goodfriend and Magaritz* [1988] showed that formation of calcite horizons in loess soils is related to the amount of rainfall. Nonetheless, calcium carbonate is the predominant mineral (20 to 49%) in most loess soils in the Negev. We show that the 220 mm precipitation isohyet, the threshold of gypsum occurrence in loess, crosses the central part of the Gaza Strip (Figure 1a). Thus we argue that the sulfate enrichment in groundwater in the south is a result of gypsum dissolution in the overlying loess, which also reflects the aridity of the area.

[30] The inverse relationship between $\delta^{13}C$ and HCO_3 values (Figure 13; data are from *Magaritz et al.* [1984]) suggests that dissolved bicarbonate is controlled by mixing of a HCO_3-rich source with low $\delta^{13}C$ values ($\sim -15‰$) in the northern part and a HCO_3-poor end-member with higher $\delta^{13}C$ values in the southern part of the aquifer. This geographical distinction in $\delta^{13}C$ and HCO_3/SO_4 ratios of groundwater mimics the $\delta^{13}C$ composition of pedogenic carbonates in overlying loess soil [*Goodfriend and Magaritz*, 1988] and the thickness of the carbonate horizon in the soil that decreases with aridity toward the south [*Dan and Yaalon*, 1982]. *Goodfriend and Magaritz* [1988] showed a north-south trend of $\delta^{13}C$ values in carbonate horizons, ranging from $\sim -10‰$ in the north to 0‰ in the south. This trend was explained by the climatic conditions; in wet conditions plant productivity increases and so the $\delta^{13}C$ in soil CO_2 decreases. It was also argued that under drier conditions the fraction of C_4 plants increases and so the $\delta^{13}C$ values. In short, we argue that the unique geographical isotopic and geochemical trends observed in the groundwater reflect the compositions of the overlying loessial deposits. In the following sections we will provide additional evidence for the two alternative scenarios, followed by a detailed discussion on the boron anomaly that is associated with the Na-rich groundwater.

5.2.1. Base Exchange Reactions Within the Aquifer

[31] According to the first scenario, dissolution of pedogenic carbonates and gypsum produced Ca-rich solutions that were recharged into the aquifer. In order to test this hypothesis we performed a mass balance calculation for the major dissolved ions (Table 4) that is based on the following assumptions: (1) the initial saline water has the composition of the typical saline Eocene groundwater without any anthropogenic contribution (e.g., Haluza well, which is

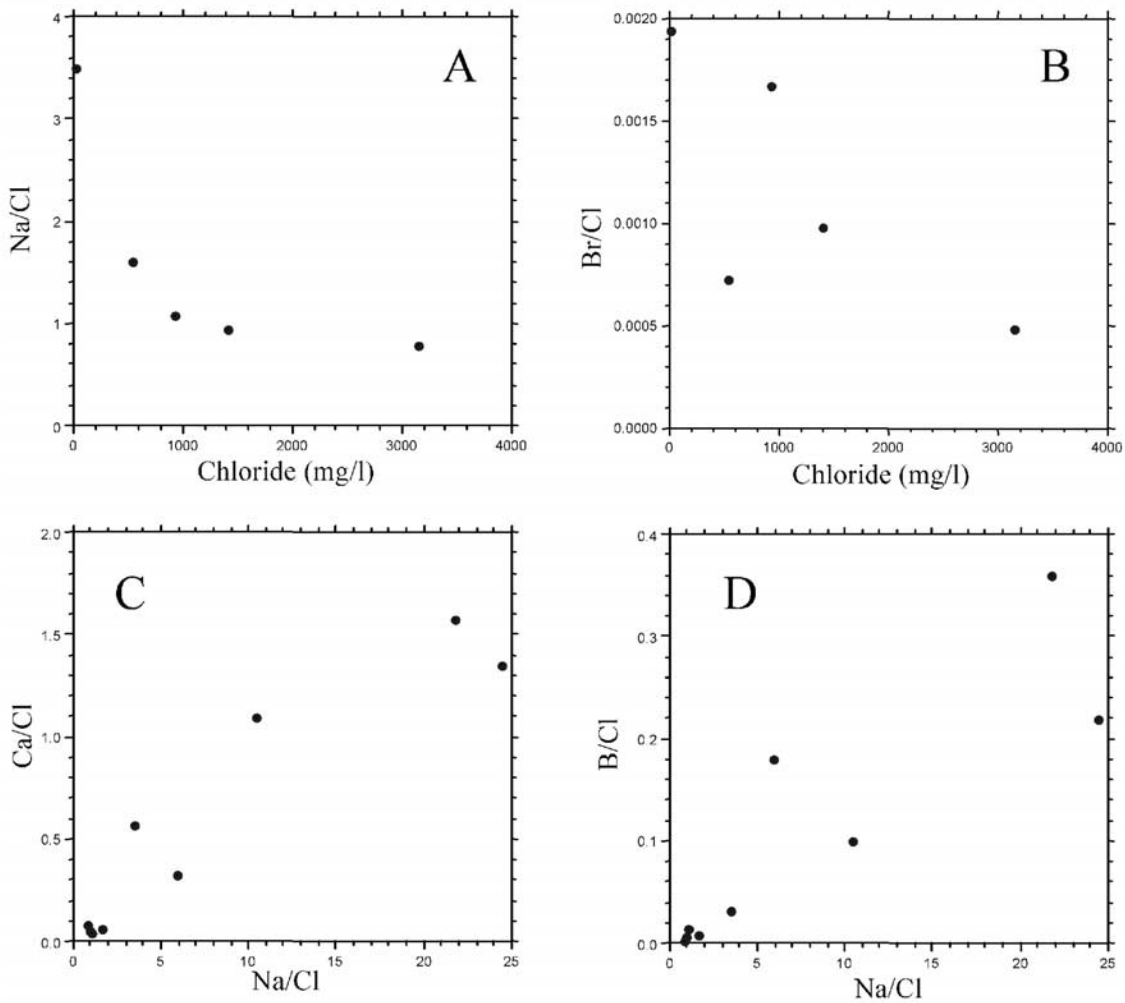

Figure 12. Results of water leaching extraction of loess soils from the northern Negev: (a) Na/Cl versus chloride (mg/L); (b) Br/Cl versus chloride; (c) Ca/Cl versus Na/Cl; and (d) B/Cl versus Na/Cl ratios.

located south of the industrial zone and hence is not influenced by its contamination; Table 1); (2) chloride is a conservative element and halite dissolution is negligible in this system given the marine Br/Cl ratios that were observed in most of the groundwater from the central part of the aquifer; (3) the dilution of Cl^- observed in the Na-rich groundwater relative to the Avedat aquitard should equally reduce the content of other dissolved ions; (4) the expected concentration of any ion normalized to that of chloride (i.e., conservative dilution) minus the actual measured concentration of those ions in the residual water equals to the net gain or loss of the ion (Δ in Table 4); and (5) the ΔHCO_3 and ΔSO_4 values represent net contribution from $CaCO_3$ and $CaSO_4$ dissolution, respectively.

[32] The results of this model (Table 4) show a significant Na^+ enrichment that is associated with Ca^{2+} depletion, HCO_3^- enrichment (northern section) and SO_4^{2-} enrichment (southern section) relative to the expected conservative concentrations. We posit that base exchange reactions are a possible explanation for the relative Na^+ addition and Ca^{2+} depletion, and therefore the net addition of Na^+ (ΔNa) should be equal to the net Ca^{2+} loss. The calcium input is the sum of Ca^{2+} in the original Eocene groundwater ($Ca_{original}$ - corrected for dilution) plus dissolution of calcite represented by the net addition of HCO_3 ($Ca_{\Delta HCO3}$) plus dissolution of gypsum as represented by the net addition of sulfate ($Ca_{\Delta SO4}$). The calcium output is the net Na enrichment (ΔNa) plus the residual Ca^{2+} concentration that is measured in the groundwater ($Ca_{residual}$). Hence the overall relationship should be (equivalent concentrations):

$$Ca_{original} + Ca_{\Delta HCO3} + Ca_{\Delta SO4} = \Delta Na + Ca_{residual}. \quad (2)$$

The results (Table 4 and Figure 14) show that in some samples, particularly the diluted one, there is a good agreement between the calculated calcium contribution (Ca input) to the net addition of Na+ plus residual Ca^{2+} (Ca output). The mass balance calculations (Table 4) show that even if Mg in the groundwater is depleted relative to the postulated diluted Eocene groundwater, the absolute magnitude of this depletion is low (1–2 meq/L), so that it does not contribute to the overall bivalent balance.

5.2.2. Base Exchange Reactions in the Overlying Loess Soil

[33] The second scenario considers base exchange reactions in the loess soil. Previous investigation of the loessial

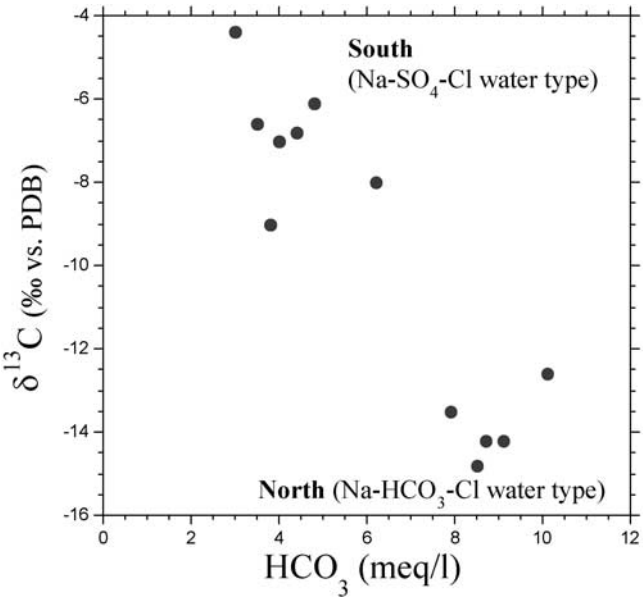

Figure 13. Values of $\delta^{13}C$ versus bicarbonate (meq/L) in Na-rich groundwater from the central part of the aquifer. Data are from *Magaritz et al.* [1984]. Note the distinction between the Na-HCO_3 type depleted in ^{13}C in the northern part and Na-SO_4 types enriched in ^{13}C in the southern part of the research area.

sequences in the Negev suggested that base exchange reactions occurred along the loess profile [*Dan and Yaalon*, 1982; *Magaritz et al.*, 1988]. We use the data reported by *Dan and Yaalon* [1982] in two loessial sequences to demonstrate this process. Figure 15 shows the chemical variations in two loessial sequences from Gilat and Beer Sheva with annual mean precipitation of 220 mm and 180 mm, respectively. The data show that in the arid area the water extractions from the loess soil are much more saline. Moreover, the relationships between Na/Cl, SO_4/Cl, and Ca/Cl ratios clearly show that gypsum dissolution (increase of SO_4/Cl and Ca/Cl) is associated with reverse base exchange reaction (an increase in Na/Cl ratios; Figure 15). The data obtained in this study also show a direct correlation between Na/Cl and Ca/Cl in the loess leachates (Figure 12). Thus the data suggests that the dissolution of carbonate and gypsum provides a large calcium pool that triggers displacement of Na^+ from exchangeable sites on clay minerals, which composed about 20% of the loessial sequences [*Magaritz et al.*, 1988]. We posit that during arid periods, salts are accumulated and stored in the loess soil. During humid phases, the soluble salts (mainly NaCl) are flushed downward and the exchange sites become saturated with Na+, followed by dissolution of less soluble minerals (calcite and gypsum), which contribute Ca^{2+} to the residual water. The calcium flux results in a reverse base

Table 4. Results of Mass Balance Calculations for the Wells in the Central Coastal Aquifer[a]

Well	Dilution Factor	Ca*, meq/L	ΔCa, meq/L	Mg*, meq/L	ΔMg, meq/L	Na*, meq/L	ΔNa, meq/L	SO4*, meq/L	ΔSO_4, meq/L	HCO_3*, meq/L	ΔHCO_3, meq/L	Net Ca Input, meq/L	Net Ca output
Central North													
Kfar Aza 2	0.5	7.1	−5.1	6.6	−1.7	26.5	19.1	5.3	4.6	1.6	6.5	18.2	21.0
Nahal Oz 2	0.5	6.6	−5.1	6.2	−2.2	24.6	19.6	4.9	2.8	1.5	6.3	15.7	21.1
Nir Am 13	0.2	2.7	−1.2	2.6	0.8	10.3	8.5	2.0	0.7	0.6	6.9	10.4	10.1
Nahal Oz 1	0.5	6.8	−5.5	6.4	−2.5	25.4	20.5	5.1	2.5	1.5	8.1	17.4	21.9
Nahal Oz 2	0.6	7.7	−6.1	7.3	−1.7	29.1	18.3	5.8	5.3	1.7	5.7	18.7	19.9
Kefar Aza 2	0.5	7.0	−5.0	6.6	−1.4	26.4	17.9	5.3	3.4	1.6	6.6	17.1	19.9
Nir Am 13	0.2	2.8	−1.2	2.7	0.9	10.7	9.2	2.1	1.0	0.6	7.2	11.1	10.9
Nir Am 10	0.1	1.6	−0.2	1.5	1.1	5.9	6.2	1.2	0.3	0.4	6.0	7.9	7.5
Nir Am 14A	0.1	1.7	0.0	1.5	1.2	6.2	4.7	1.2	0.04	0.4	5.0	6.7	6.4
Nir Am 17A	0.1	1.6	0.5	1.5	1.3	6.1	4.4	1.2	−0.01	0.4	5.6	7.2	6.5
Shokeda 6	0.4	5.9	−3.9	5.6	−0.7	22.3	14.4	4.5	4.3	1.3	5.9	16.2	16.4
Shoqeda 6	0.4	6.1	−4.0	5.7	−0.9	22.8	15.5	4.5	3.3	1.4	5.7	15.1	17.6
Alumim 2	0.8	10.5	−5.6	9.9	2.6	39.4	19.5	7.9	6.5	2.4	3.1	20.2	24.4
Central South													
Moshavei Negev 2	0.6	7.7	−2.9	7.2	−0.6	28.8	12.7	5.8	7.3	1.7	1.7	16.7	17.5
Nirim 2	0.3	4.6	−0.1	4.4	1.1	17.5	4.3	3.5	3.3	1.0	1.4	9.3	8.9
Moshavei Negev 2	0.6	8.0	−3.5	7.5	−0.9	29.9	19.5	6.0	7.4	1.8	1.3	16.7	23.9
Re'im 1	0.3	3.5	−0.5	3.2	1.0	13.0	7.0	2.6	2.3	0.8	3.2	9.0	10.0
Nirim 2	0.3	4.6	0.4	4.3	1.2	17.4	6.1	3.5	3.0	1.0	1.7	9.4	11.1
Khesufim 2	0.6	7.7	−3.2	7.2	−0.8	28.9	13.0	5.8	28.4	1.7	−1.7	34.4	17.5
Nirim 5	0.5	7.1	−3.7	6.7	−1.4	26.7	17.1	5.4	11.0	1.6	1.6	19.7	20.5
Moshaviei Hanegev 2	0.6	7.7	−3.0	7.2	−0.1	28.9	11.4	5.8	5.4	1.7	2.1	15.2	16.1
Nirim 2 saline	0.2	3.2	−1.9	3.0	−0.8	11.9	13.5	2.4	4.7	0.7	4.2	12.2	14.9
Nirim 4	0.3	4.5	−2.4	4.2	−0.7	16.9	14.8	3.4	7.2	1.0	2.9	14.6	16.8
Nirim 5	0.5	6.6	−3.4	6.2	−1.3	24.9	17.6	5.0	9.0	1.5	2.1	17.8	20.9
Shoqeda 2	0.7	9.4	−4.8	8.8	3.3	35.2	13.5	7.0	8.2	2.1	3.3	20.9	18.2
Reim 1	0.3	3.9	−0.5	3.7	1.0	14.7	5.4	2.9	2.0	0.9	3.2	9.2	8.9
Reim 1	0.3	3.9	−0.5	3.7	0.9	14.8	4.7	2.9	1.5	0.9	3.3	8.7	8.2

[a]The content of each ion, marked with an asterisk (in meq/L), was calculated assuming that the Eocene groundwater from the Avedat Group aquitard was diluted and chloride was preserved to reflect this dilution. The difference between calculated values and measured values of each ion (Table 1) are marked as "Δ".

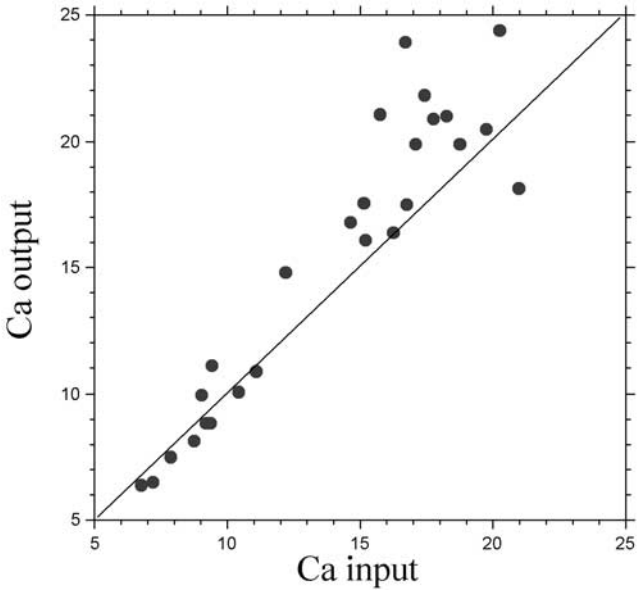

Figure 14. Results of the mass balance calculations for the "Ca input" deduced from diluted Eocene calcium, ΔHCO_3, and ΔSO_4 values (see text and Table 4) and "Ca output" calculated from the relative enrichment of Na (ΔNa) and the residual Ca^{2+} measured in the groundwater (in meq/L).

exchange reaction and, according to this scenario, generates a Na-rich solution that is recharged into the saturated part of the aquifer.

5.2.3. Boron Anomaly

[34] The Na-rich saline groundwater in the central part of the southern coastal aquifer is characterized by high boron concentrations (up to 4.3 mg/L, Table 1) and extremely high B/Cl ratios (1×10^{-2} relative to 8×10^{-4} in seawater). The boron isotopic ratios reflect mixing between two sources: (1) saline groundwater with high δ^{11}B values (~48‰); and (2) fresh groundwater with low δ^{11}B values (~25‰; Figure 8). Treated wastewater is transported from the Dan Region Reclamation Project in the central coastal aquifer and used for irrigation over the southern coastal aquifer. Thus one could suggest that the boron anomaly is derived from infiltration of boron-rich wastewater. However, the high δ^{11}B values (~48‰) obtained in the saline groundwater rule out this possibility as wastewater from the Dan Region Reclamation Project has a δ^{11}B range of 0 to 10‰ [*Vengosh et al.*, 1994]. While the δ^{11}B values of the Na-rich saline groundwater in the center of the aquifer (~48‰) are not much different from the Avedat Group groundwater (~45‰, Rosenberg, personal communication), the boron content is much higher. The increase of B/Cl ratios is correlated with that of Na/Cl ratios in both the saline groundwater (Figure 10) and loess leachates (Figure 12), suggesting a common origin. Given these relationships and the extremely high B/Cl ratios found in the loess extractions, we suggest that the source of boron anomaly in the groundwater is related to processes in the overlying loess. Our findings show that the loess leachates have high B/Cl and low δ^{11}B values of 17 to 31‰ (Table 3 and Figure 16). As shown in Figure 12, the saline leachates have low Br/Cl ratios that indicate halite dissolution. Hence the B/Cl ratios in the loess extraction also reflect the contribution of halite dissolution with a negligible amount of boron [*Vengosh et al.*, 1994], that is, extremely low B/Cl ratios. In spite of the halite contribution, the B/Cl ratios in the loess extractions are high, which indicates a significant boron-rich source. We suggest that leaching of the loess soil extracts "desorbable boron" from clay minerals given that "desorbable boron" in marine sediments has a δ^{11}B range of 15‰ to 20‰ [*Spivack et al.*, 1987]. The relationships between boron in loess leachates and saline groundwater (Figure 16) suggest that the high B and low δ^{11}B source was modified into slightly lower B and higher δ^{11}B via adsorption process, most probably within the saturated zone. A well-known feature of clay minerals is their high adsorption capacity with respect to boron [*Spivack et al.*, 1987; *Palmer and Swihart*, 1996]. We suggest that long-term accumulation of marine aerosols with δ^{11}B ~ 39‰ in the loess deposits resulted in an

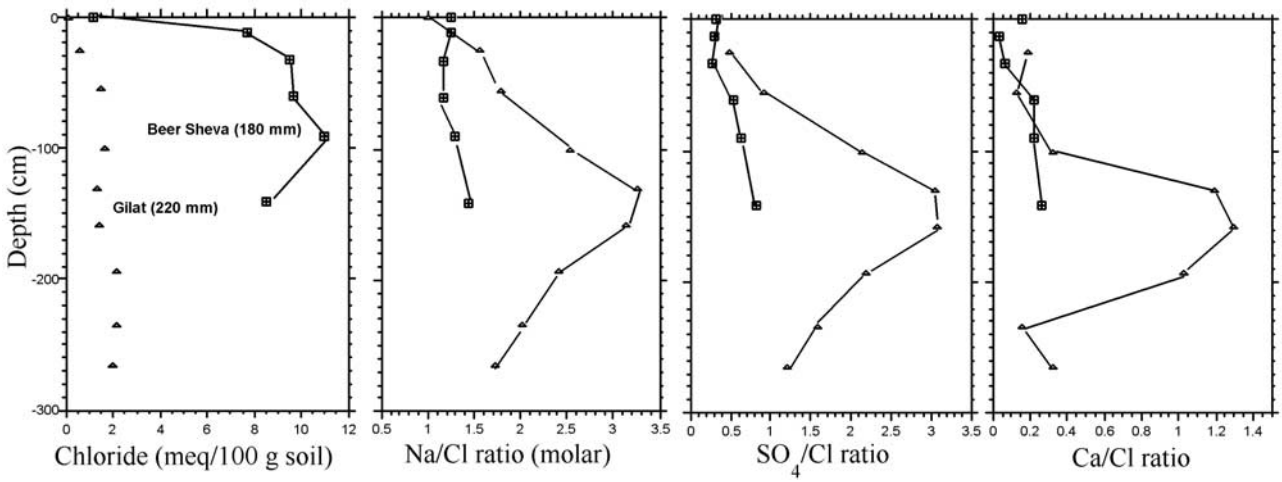

Figure 15. Variations of chloride, Na/Cl, SO_4/Cl, and Ca/Cl values in two loessial sequences in the northern Negev (Gilat and Be'er Sheva sites). Data are from *Dan and Yaalon* [1982]. Note that the peak in SO_4/Cl in Gilat section is associated with Ca/Cl and Na/Cl ratios, indicating that gypsum dissolution triggered reverse base exchange reactions.

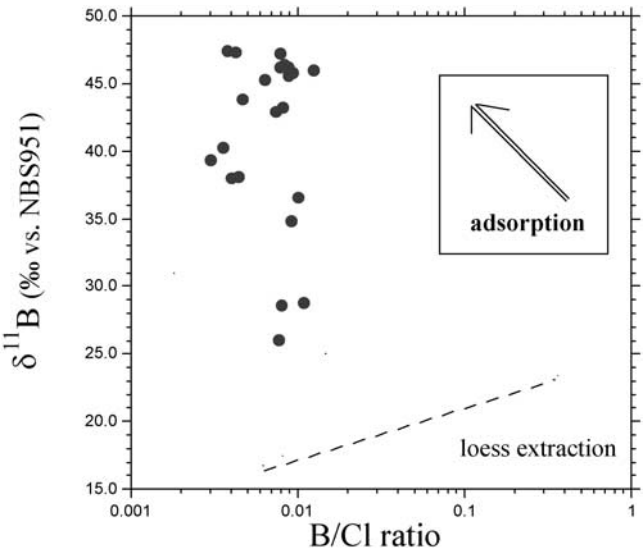

Figure 16. Values of $\delta^{11}B$ versus B/Cl (molar) ratios measured in the loess leachates and the saline Na-rich groundwater. The high B/Cl ratio found in the loess leachates is associated with lower $\delta^{11}B$ values relative to that of the underlying groundwater. Adsorption of boron onto clay minerals is one of the most probable mechanisms for a shift from high B/Cl and low $\delta^{11}B$ to relatively lower B/Cl and high $\delta^{11}B$ values.

equilibrium between the dissolved (>39‰) and adsorbed (<39‰) boron phases. The boron-rich solution percolated into the saturated zone and a new equilibrium condition with the host clay minerals was established, in which the residual groundwater became enriched in ^{11}B upon selective removal of ^{10}B to the adsorbed phase.

5.3. Sources of Salinization in the Gaza Strip

[35] While groundwater in the central part of the aquifer has a long record of high salinity that was already observed during the 1930s [*Mercado*, 1968; *Fink*, 1992; *Melloul and Bibas*, 1992], salinization in the western part of the southern coastal aquifer, that is the Gaza Strip, is an ongoing process [*Moe et al.*, 2001].

[36] Our findings indicate three major sources of salinity that affect the water quality in the Gaza Strip. The first is lateral flow of Na-rich saline groundwater from the central part of the aquifer, (2) seawater intrusion, and (3) anthropogenic nitrate pollution. The chemical (Figure 5), oxygen (Figure 6) and boron isotopic compositions (Figure 8) of the saline groundwater in the Gaza Strip indicate that most of the salinity is derived from the lateral flow of Na-rich saline groundwater from the central section of the aquifer. The lithological composition of the unsaturated zone is changing from loess-dominant soil in the eastern part to sandstone with high permeability in the western area. This transition occurs along the Israel-Gaza Strip border (Figure 3). As a result, the saline groundwater in the central aquifer becomes less saline as it flows to the Gaza Strip. Nevertheless, the unique chemical composition (e.g., high Na/Cl and B/Cl) is only slightly modified (Figure 5) and the chemical composition of groundwater in the central and eastern parts of the Gaza Strip mimics the composition of the Na-rich groundwater in the Israeli side. This observation is generally consistent with that of *Fink* [1992], who estimated that the lateral groundwater flow from the Israeli side to the Gaza Strip is 37×10^6 m^3/y, which is about one third of total replenishment of $\sim 120 \times 10^6$ m^3/y. Since water levels within the Gaza Strip have dropped during the last three decades due to overpumping, we suggest that the SE-NW groundwater gradient has become steeper, and as a consequence, the flow rate of the saline groundwater should have increased, resulting in the salinization of the groundwater in the Gaza Strip.

[37] The second source of salinity that was identified in several wells is seawater intrusion that is characterized by a marine Br/Cl ratio, low Na/Cl (<0.86), B/Cl, SO_4/Cl ratios, and high Ca/Cl and $\delta^{11}B$ values. The high Ca/Cl ratios observed in the seawater intrusion samples are also positively correlated with $^{87}Sr/^{86}Sr$ ratios (Figure 11), which indicates that the Sr^{2+} that is released from clay minerals during base exchange reactions has a high $^{87}Sr/^{86}Sr$ ratio. A similar trend was shown in Salinas Valley, California, where saline groundwater associated with seawater intrusion has both high Ca and $^{87}Sr/^{86}Sr$ ratios relative to local groundwater [*Vengosh et al.*, 2002].

[38] The third source is anthropogenic contamination. The results of a numerical model in the northern part of the Gaza Strip [*Weinthal et al.*, 2005] indicate that anthropogenic contribution to the salt budget is only 10% although recharge from the aquifer surface contributes 37% of the water balance. Hence the anthropogenic contamination has negligible affect on the salinity. However, we found extremely high levels of nitrate in groundwater from the Gaza Strip. While groundwater in the Israeli side has low nitrate concentrations (<30 mg/L; as NO_3), the level of nitrate in the groundwater within the Gaza Strip can reach 450 mg/L. We postulate that the source of the nitrate in the groundwater is derived from agricultural return flow and/or wastewater pollution and nitrification processes in the unsaturated zone of the aquifer. While the saline groundwater that flows into the Gaza Strip is particularly low in Ca^{2+}, Mg^{2+}, together with low $^{87}Sr/^{86}Sr$ ratios, within the Gaza Strip itself we observed high Ca^{2+} and Mg^{2+} contents, as well as relatively high $^{87}Sr/^{86}Sr$ ratios (Figure 7). The increase of Ca^{2+} tends to correlate with that of magnesium, nitrate, and $^{87}Sr/^{86}Sr$ ratios (Figure 11). We suggest that the chemical and strontium isotopic changes observed within the Gaza Strip are related to the nitrate pollution process. During the nitrification process, microbial oxidation of ammonium releases protons (H^+) that generate acidity along with nitrate in soils [*Bölke*, 2002] and induce dissolution of calcium carbonate minerals. In many carbonate aquifers nitrate-rich waters are associated with high calcium derived from dissolution of the aquifer matrix [*Bölke*, 2002]. Moreover, groundwater recharged beneath fertilized fields has a unique Ca-Mg-NO_3 composition with positive correlations between nitrate and other inorganic constituents like Mg^{2+}, Ca^{2+}, Sr^{2+}, Ba^{2+}, K^+ and Cl^- [*Hamilton and Helsel*, 1995]. Since the matrix of the sandstone in the coastal aquifer is composed of high Mg calcite [*Gavish and Friedman*, 1969], we suggest that the nitrification process induced dissolution of the carbonate matrix. Furthermore, we argue that the conspicuous increase of the $^{87}Sr/^{86}Sr$ ratios indicates a contribution of the Pleistocene

carbonate matrix ($^{87}Sr/^{86}Sr \sim 0.7090$) and that $^{87}Sr/^{86}Sr$ ratio is not directly derived from nitrate sources but rather from water-rock interactions.

6. Conclusions: Conservative Tracers and the Distinction of Natural From Anthropogenic Salinity Sources

[39] The use of hydrochemical fingerprints for tracing the origin of salinity of groundwater resources is a very powerful methodology that enables identification of multiple salinity sources in coastal aquifers [*Vengosh*, 2003, and references therein]. The basic assumption for this technique is that the chemical and isotopic compositions of the saline source are preserved during the salinization process (i.e., the geochemical tracers are conservative). Thus it is expected that the chemical composition of the salinized water would mimic the original saline source. However, water-rock interactions may mask and even modify the original chemical composition. Here, we showed a significant chemical modification of downgradient groundwater in the central part of the Mediterranean coastal aquifer relative to the original saline source in the adjacent Avedat Group aquitard. The integration of geochemical and isotopic tracers enabled us to show that the major source of the water is derived from lateral flow from the underlying Avedat aquitard (as inferred from $\delta^{18}O$ and $\delta^{2}H$ values), while the *solutes* are derived from water-rock interactions, primarily in the overlying loess soil. We use the "refreshening" concept [*Appelo*, 1994] to suggest that the unique $Na\text{-}HCO_3\text{-}Cl$ and $Na\text{-}SO_4\text{-}Cl$ compositions found in saline groundwater in the central aquifer are a product of reverse base exchange reactions. We argue that the overlying soil is an undistinguishable source for dissolved calcium given the abundance of pedogenic carbonates and gypsum. We postulate two models for the base exchange reactions; one considers in situ reactions in the aquifer due to flux of Ca-rich solution from the overlying loess. The second suggests that base exchange reactions occur within the loessial sequence. Thus the apparent inconsistency of continuous groundwater flow and the dramatic change in water chemistry can be resolved by considering the role of water-rock interactions together with mixing processes.

[40] The geochemical data indicate that the ongoing salinization process within the Gaza Strip is largely derived from the lateral flow of saline groundwater from the central part of the aquifer. Here again, the main source of the salinity is natural ("geogenic") and not derived from anthropogenic sources. Nonetheless, the high nitrate contents found in groundwater within the Gaza Strip and the associated changes in water chemistry (e.g., the increase of Ca^{2+} and $^{87}Sr/^{86}Sr$) clearly indicate an anthropogenic component of pollution. Hence the water quality in the Gaza Strip is affected by natural saline sources (eastern Na-rich groundwater and seawater intrusion) superimposed with anthropogenic nitrate-rich contamination. In addition, the high Br groundwater found in the alluvial shallow aquifer along the Wadi Besor (Gaza) is a sign of industrial pollution.

[41] The use of geochemical tools to delineate the source of salinity has important political implications for future management and potential cooperation between Israel and the Palestinian Authority. In particular, the local water authorities can use these geochemical tools to establish a reliable monitoring program that can identify the multiple salinity sources.

[42] Salinization by the lateral flow of the Na-rich groundwater turns out to be the predominant factor for the salinity rise in the eastern and central parts of the Gaza Strip. This finding should be taken into account in future management scenarios since it could be the basis for strategies to reduce the eastern saline flux and thus slow down salinization in the Gaza Strip or even reverse the tendency and improve the overall quality of the groundwater resources [*Weinthal et al.*, 2005].

[43] **Acknowledgments.** This study is part of the BOREMED project (contract EVK1-CT-2000-00046) cofinanced by the European Union under the 5th Framework Program. We appreciate and thank the Associate Editor and two anonymous reviewers for a thorough and enlightening review that significantly improved the quality of this manuscript.

References

Adar, E., and R. Nativ (2003), Isotopes as tracers in a contaminated fractured chalk aquitard, *J. Contam. Hydrol.*, *65*, 19–39.

Appelo, C. A. J. (1994), Cation and proton exchange, pH variations, and carbonate reactions in a freshening aquifer, *Water Resour. Res.*, *30*, 2793–2805.

Assaf, S. A. (2001), Existing and the future planned desalination facilities in the Gaza Strip of Palestine and their socio-economic and environmental impact, *Desalination*, *138*, 17–28.

Bölke, J. K. (2002), Groundwater recharge and agricultural contamination, *Hydrogeol. J.*, *10*, 153–179.

Dan, J., and D. H. Yaalon (1982), Automorphic saline soils in Israel, *Catena Suppl.*, *1*, 103–115.

Epstein, S., and T. Mayeda (1953), Variation of ^{18}O content of waters from natural sources, *Geochim. Cosmochim. Acta*, *4*, 213–224.

Fink, M. (1970), Hydrogeology of the Gaza Strip (in Hebrew), *Report HG/70/07*, Tahal Co. Ltd., Tel Aviv, Israel.

Fink, M. (1992), An update of the hydrological situation in the Gaza Strip–1992 (in Hebrew), *Rep. 04/92/45*, Tahal Co. Ltd., Tel Aviv, Israel.

Gaillardet, J., and C. J. Allègre (1995), Boron isotopic compositions of corals: Seawater or diagenesis record?, *Earth Planet. Sci. Lett.*, *136*, 665–676.

Gavish, E., and G. M. Friedman (1969), Progressive diagenesis in Quaternary to Late Tertiary carbonate sediments: Sequence and time scale, *J. Sediment. Petrol.*, *39*, 980–1006.

Goodfriend, G. A., and M. Magaritz (1988), Palaeosols and late Pleistocene rainfall fluctuations in the Negev Desert, *Nature*, *332*, 144–146.

Guttman, J. (2002), Producing brackish water from the Pleistocene and Judea Group aquifers in the northern Negev (in Hebrew), *Rep. 733*, Mekorot, Tel Aviv, Israel.

Gvirtzman, G. (1969), The Saqiye group (late Eocene to early Pleistocene) in the Coastal Plain and Hashphela regions, Israel, *Geol. Surv. Isr. Bull.*, *51*, 2.

Hamilton, P. A., and D. R. Helsel (1995), Effects of agriculture on groundwater quality in five regions of the United States, *Ground Water*, *33*, 217–226.

Issar, A., D. Bahat, and E. Wakshal (1988), Occurrence of secondary gypsum veins in joints in chalks in the Negev, Israel, *Catena*, *15*, 241–247.

Izbicki, J. A. (1991), Chloride sources in a California Coastal Aquifer. Ground water in the Pacific Rim countries, paper presented at American Society of Consulting Engineers Conference, Honolulu, Hawaii, 23–35 July.

Jones, B. F., A. Vengosh, E. Rosenthal, and Y. Yechieli (1999), Geochemical investigations, in *Seawater Intrusion in Coastal Aquifers: Concepts, Methods and Practices*, edited by J. Bear et al., pp. 51–72, Springer, New York.

Kelly, K., and T. Homer-Dixon (1998), Environmental scarcity and violent conflict: The case of Gaza, in *Ecoviolence: Links Among Environment, Population, and Security*, edited by H. Homer-Dixon and J. Blitt, pp. 67–108, Rowman and Littlefield, Lanham, Md.

Keshet, N. (1992), Contamination along Besor and Beer Sheva rivers. Monitoring results 1990/92 (in Hebrew), 33 pp., Isr. Nat. Prot. Auth., Jerusalem.

Keshet, N. (1999), Contamination along Besor and Beer Sheva rivers. Monitoring results 1998/99 (in Hebrew), 29 pp., Isr. Nat. and Natl. Parks Prot. Auth., Jerusalem.

Livshitz, Y. (1999), Influence of natural and artificial factors on the chemical composition of groundwater in the north-western Negev and the southern portion of the HaShefela region, Israel (in Hebrew), Ph.D. thesis, 146 pp., Ben Gurion Univ., Beer Sheva, Israel.

Magaritz, M., A. Nadler, U. Kafri, and A. Arad (1984), Hydrochemistry of continental brackish waters in the southern coastal plain, Israel, *Chem. Geol.*, *42*, 159–176.

Magaritz, M., H. Gvitzman, and A. Nadler (1988), Salt accumulation in the loessial sequence in the Be'er Sheva basin, Israel, *Environ Geol. Water Sci.*, *11*, 27–33.

Maslia, M. L., and D. C. Prowell (1990), Effects of faults on fluid flow and chloride contamination in a carbonate aquifer system, *J. Hydrol.*, *115*, 1–49.

Melloul, A., and M. Bibas (1992), Hydrological situation in the coastal aquifer of Gaza Strip from 1985 to 1990 (in Hebrew), *Rep. 1992/7*, Hydrol. Serv., Jerusalem, Israel.

Mercado, A. (1968), A hydrological survey of groundwater in the Gaza Strip (in Hebrew), *Rep. 1968*, Tahal Co. Ltd., Tel Aviv, Israel.

Michaeli, A., and M. Movshoviz (1981), Gevulot drainage and Besor River (in Hebrew), report, 7 pp., Tahal Co. Ltd., Tel Aviv, Israel.

Moe, H., R. Hossain, R. Fitzgerald, M. Banna, A. Mushtaha, and A. Yaqubi (2001), Application of a 3-dimensional coupled flow and transport model in the Gaza Strip, paper presented at the First International Conference on Saltwater Intrusion and Coastal Aquifers—Monitoring, Modeling, and Management, Int. Assoc. of Hydraul. Eng. and Res., Essaouira, Morocco, 23–25 April.

Movshoviz, M. (1979), The Besor drainage (in Hebrew), report, 16 pp., Tahal Co. Ltd., Tel Aviv, Israel.

Nativ, R., and E. Adar (1997), Estimation of groundwater contamination in Ramat-Hovav area. Summary of activity in 1995–1997 (in Hebrew), report, 81 pp., Ramat-Hovav Ind. Counc., Ramat Hovav, Negev, Israel.

Nativ, R., and I. Nissim (1992), Characterization of desert aquitard—Hydrologic and hydrochemical considerations, *Ground Water*, *30*, 598–606.

Nativ, R., E. Adar, O. Dahan, and M. Geyh (1995), Water recharge and solute transport through the vadose zone of fractured chalk under desert conditions, *Water Resour. Res.*, *31*, 253–261.

Négrel, P., and P. Deschamps (1996), Natural and anthropogenic budgets of a small watershed in the Massif Central (France): Chemical and strontium isotopic characterization of water and sediments, *Aquat. Geochem.*, *2*, 1–27.

Ohlsson, L. (1995), *Hydropolitics*, 230 pp., Zed Books, London.

Oshumi, T., and H. Fujini (1986), Isotope exchange technique for preparation of hydrogen gas in mass spectrometric D/H analysis of natural waters, *Anal. Sci.*, *2*, 489–490.

Palmer, M. R., and G. H. Swihart (1996), Boron isotope geochemistry: An overview, in *Boron: Mineralogy, Petrology, and Geochemistry*, edited by E. S. Grew and L. M. Anovitz, *Rev. Mineral.*, *33*, 709–744.

Penny, E., M.-K. Lee, and C. Morton (2003), Groundwater and microbial processes of the Alabama coastal plain aquifers, *Water Resour. Res.*, *39*(11), 1320, doi:10.1029/2003WR001963.

Spivack, A. J., and J. M. Edmond (1986), Determination of boron isotope ratios by thermal ionization mass spectrometry of the dicesium metaborate cation, *Anal. Chem.*, *58*, 31–35.

Spivack, A. J., M. R. Palmer, and J. M. Edmond (1987), The sedimentary cycle of the boron isotopes, *Geochim. Cosmochim. Acta*, *51*, 1939–1950.

Tolmach, Y. (1991), *Hydrogeological Atlas of Israel, Coastal aquifer and Gaza Area* (in Hebrew), 24 pp., Hydrol. Serv., Jerusalem, Israel.

Vengosh, A. (2003), Salinization and saline environments, in *Treatise in Geochemistry*, vol. 9, *Environmental Geochemistry*, edited by B. S. Lollar, pp. 333–365, Elsevier, New York.

Vengosh, A., K. G. Heumann, S. Juraske, and R. Kasher (1994), Boron isotope application for tracing sources of contamination in groundwater, *Environ. Sci. Technol.*, *28*, 1968–1974.

Vengosh, A., A. J. Spivack, Y. Artzi, and A. Ayalon (1999), Boron, strontium, and oxygen isotopic and geochemical constraints for the origin of salinity in groundwater from the Mediterranean coast of Israel, *Water Resour. Res.*, *35*, 1877–1894.

Vengosh, A., J. Gill, M. L. Davisson, and G. B. Huddon (2002), A multiisotope (B, Sr, O, H, and C) and age dating (^{3}H-^{3}He, and ^{14}C) study of groundwater from Salinas Valley, California: Hydrochemistry, dynamics, and contamination processes, *Water Resour. Res.*, *38*(1), 1008, doi:10.1029/2001WR000517.

Weinthal, E., A. Vengosh, A. Marie, A. Gutierrez, and W. Kloppmann (2005), The water crisis in the Gaza Strip: Prospects for resolution, *Ground Water*, in press.

Yechieli, Y., O. Sivan, B. Lazar, A. Vengosh, D. Ronen, and B. Herut (2001), ^{14}C in seawater intruding into the Israeli Mediterranean coastal aquifer, *Radiocarbon*, *43*(2B), 773–781.

M. Banna, Palestinian Water Authority, Gaza, Gaza Strip.

A. Gutierrez, BRGM, Water Department, 3 av. C. Guillemin, BP 6009, F-45060, Orléans cedex 2, France.

C. Guerrot, Service ANA, BRGM, 3 av. C. Guillemin, BP 6009, F-45060 Orléans cedex 2, France.

W. Kloppmann, Service EAU, BRGM, 3 av. C. Guillemin, BP 6009, F-45060 Orléans cedex 2, France.

Y. Livshitz, Hydrological Service, PO Box 6381, Jerusalem 91063, Israel.

A. Marei, Department of Applied Earth and Environmental Sciences, Al Quds University, Betany P.O. Box 89, Jerusalem, West Bank.

I. Pankratov, H. Raanan, and A. Vengosh, Department of Geological and Environmental Sciences, Ben-Gurion University of the Negev, Be'er Sheva 84105, Israel. (avnerv@bgumail.ac.il)

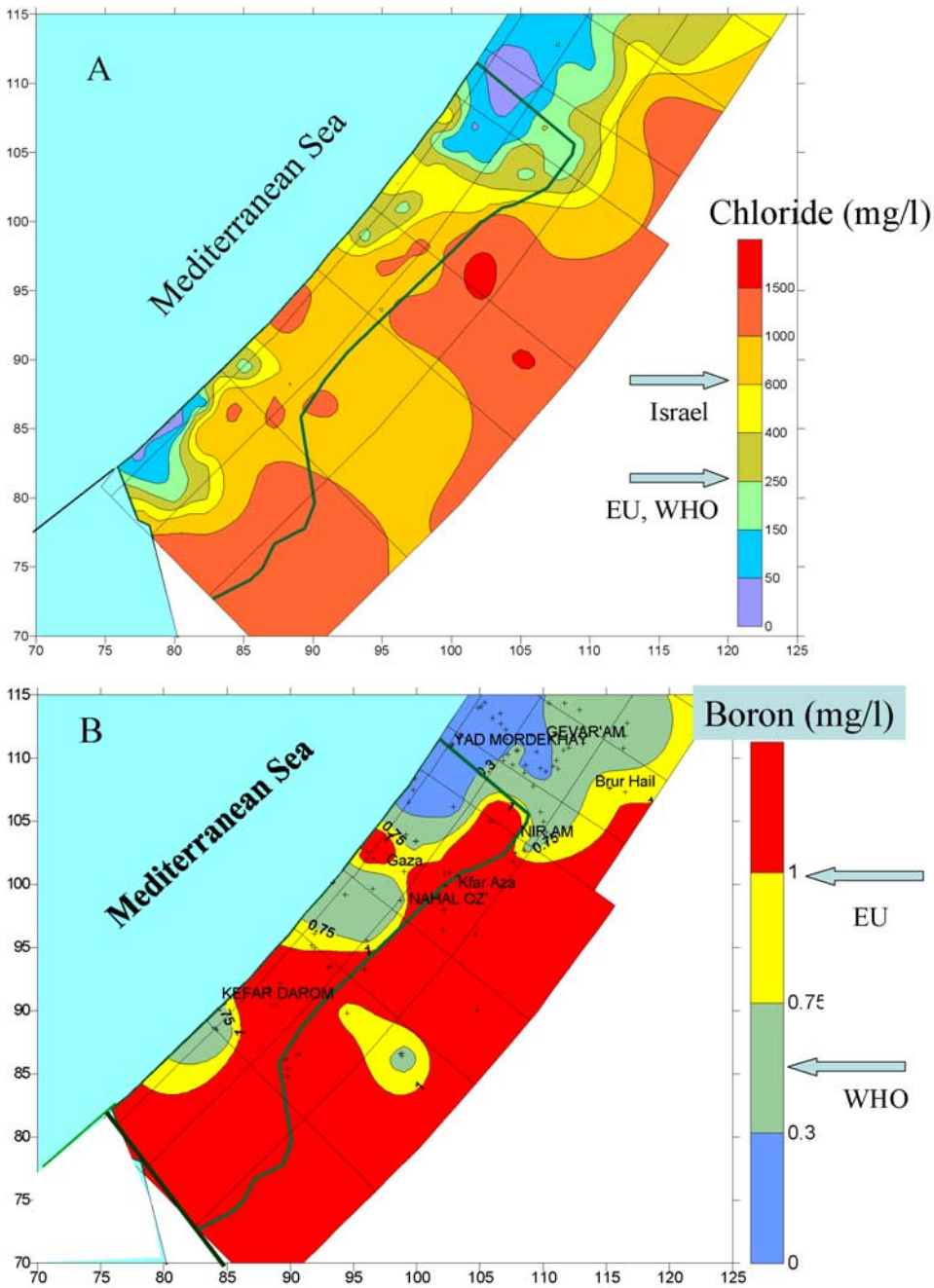

Figure 2. (a) Distribution of chloride concentrations (mg/L) in the southern Mediterranean coastal aquifer and the Gaza Strip as measured in 2000. Arrows indicate upper limits of drinking-water regulations in Israel and the European Union (EU) and recommended by the World Health Organization (WHO). (b) Distribution boron concentrations (mg/L) in the southern Mediterranean coastal aquifer and the Gaza Strip as measured in 2000. Arrows indicate upper limits of drinking water regulations in Israel and the European Union (EU) and recommended by the World Health Organization (WHO).